Chapter 5

Nonlinear Controllers (I): Based on the Partial State Feedback Linearization Technique

This chapter presents the design of nonlinear controllers for hydraulic turbines with or without surge tanks. Moreover, it proposes comparative studies where cost functions are defined and utilised to determine the advantages of these nonlinear controllers.

The chapter is organised as follows. Section 5.1 gives an introduction. Section 5.2 describes the hydraulic turbine models used for the design of nonlinear controllers. Section 5.3 presents the development of nonlinear controllers designed from nonlinear models of hydraulic turbines *with no* surge tank effects. Section 5.4 develops nonlinear controllers designed from nonlinear models of hydraulic turbines *with* surge tank effects. Section 5.5 presents load rejection studies. Finally, Section 5.6 presents the summary and conclusions of this chapter.

5.1 Introduction

PID controllers have played an important role in the control of hydraulic power plants. The main obstacle to obtain a good performance control system is that the dynamics of the plant are nonlinear and may vary greatly along with the operating point. Traditionally, these problems have been dealt with by tuning the parameters of the controller to give an acceptable response for all conditions or by using Gain Scheduling controllers (Riera and Cardoner, 1992).

This chapter presents alternative controllers that combine the nonlinear control technique called partial state feedback linearization, also input-output linearization, and PID features to cope with some of the control problems existing in these plants. Comparative studies, where the new controllers are evaluated, show the advantages and power of this technique.

Nonlinear hydraulic models of turbines with or without surge tanks are used to represent the behaviour of the plant. Four nonlinear controllers for hydraulic plants supplying isolated loads are studied and compared to PID or PI-PD controllers. Two of these controllers (NL A and NL B) are designed from a nonlinear model *with no* surge tank effects (Quiroga, Batlle and Riera, 2000). Moreover, this chapter completes that study by presenting the adjustment tables (surfaces) for the main controllers (NL B, PID and PI-PD). The two remaining controllers (NL C and NL D), are designed from a nonlinear model *with* surge tank effects, and presented in this chapter by continuing the design ideas followed in the above mentioned paper. Besides, the zero dynamics for the controllers NL A, NL B, NL C and NL D are introduced in order to prove the stability of these controllers.

Apart from this, complete studies are performed comparing these new mixed algorithms to the classical PID and PI-PD controllers. These comparisons are achieved by means of cost functions that take into account not only the output behaviour but also the control effort.

In order to understand the characteristics of the control, it is essential to explain a general control scheme of the hydraulic power plant. Hence, Figure 5.1 represents in a functional block diagram the relationship between the hydroelectric system and the *controls*: on the one hand the *speed control*, and on the other hand the *load generation control*. The frequency of a hydroelectric system depends on the balance of the active power. If a change in the active

power demand occurs, then the power balance is affected, the speed of the turbine and the frequency of the synchronous generator are also affected. In order to control the active power both control loops must be used.

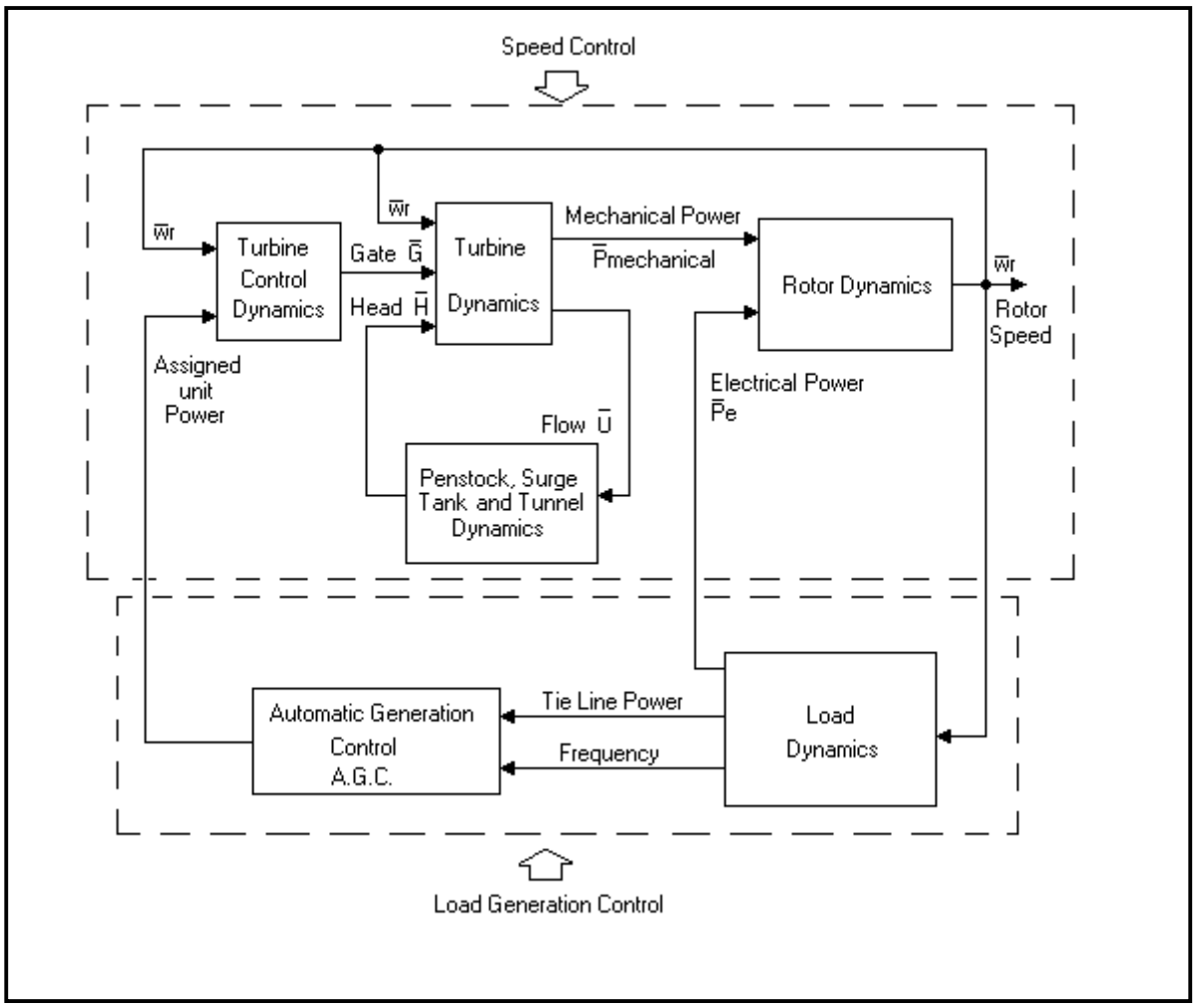

Figure 5.1: Functional block diagram showing the relation between the hydroelectric system and the controls for a complete system.

As Chapter 1 indicates, this dissertation considers in general, the case of isolated (or islanded) system operation. In particular, a hydroelectric power plant supplying an isolated load is taken into account. Figure 5.2 contemplates a general speed control scheme for a hydropower plant supplying an isolated load.

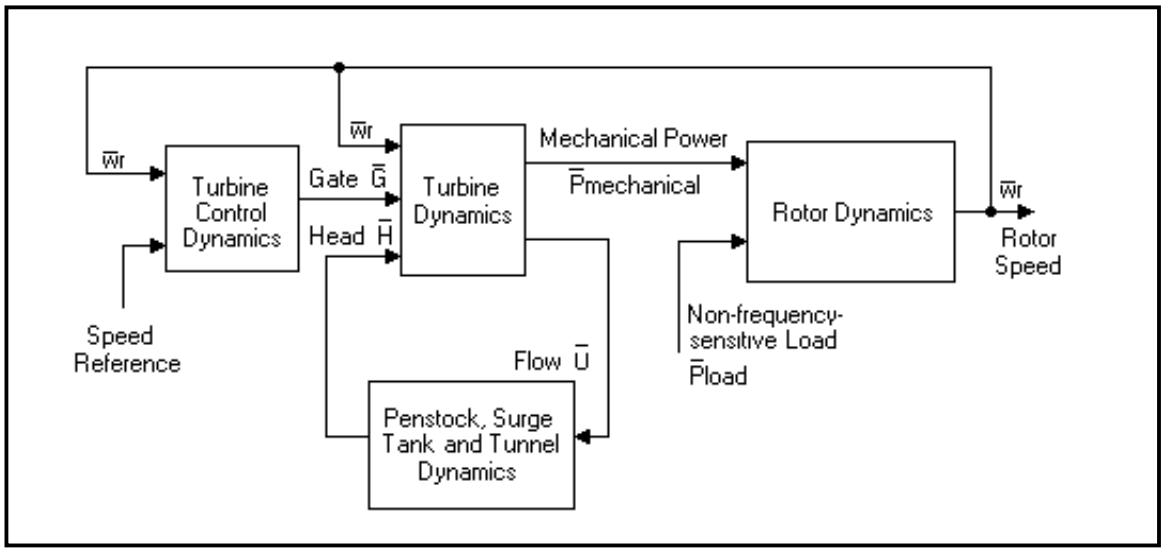

Figure 5.2: General speed control scheme for a generic controller.

5.2 Models for Hydraulic Turbines

The nonlinear model for hydraulic turbines with or without surge tanks may take into account the effects of water inertia, water compressibility and pipe wall elasticity in the penstock. The equations that compose these models (IEEE Working Group, 1992; Kundur, 1994) can be taken from Chapter 3. The model of a hydraulic turbine *with surge tank* considers non-elastic water columns (penstock and tunnel). The model of a hydraulic turbine *with no surge tank* can also consider non-elastic water column in penstock.

The dynamics of the model of a hydraulic turbine are given by:

- Dynamics of the penstock:

$$\overline{H}_l = f_p \cdot \overline{U}_t^{\,2} \tag{5. 1}$$

$$\frac{d\overline{U}_t}{dt} = \frac{\overline{H}_r - \overline{H}_t - \overline{H}_l}{T_{WP}} \tag{5. 2}$$

$$\overline{U}_t = \overline{G} \cdot \sqrt{\overline{H}_t} \tag{5. 3}$$

- Mechanical power:

$$\overline{P}_{mechanical} = A_t \cdot \overline{H}_t \cdot \left(\overline{U}_t - \overline{U}_{NL}\right) \tag{5. 4}$$

- Dynamics of the gate servomotor:

$$T_g \cdot \frac{d\overline{G}}{dt} + \overline{G} = u \tag{5. 5}$$

- Equation of motion in the turbine:

$$\overline{P}_{mechanical} - \overline{P}_{load} = 2 \cdot H \cdot \frac{d\overline{\omega}_r}{dt} + D \cdot \overline{\omega}_r \tag{5. 6}$$

- Dynamics of the tunnel:

$$\overline{H}_{l2} = f_{p2} \cdot \overline{U}_c \cdot \left|\overline{U}_c\right| \tag{5. 7}$$

$$\frac{d\overline{U}_c}{dt} = \frac{\overline{H}_0 - \overline{H}_r - \overline{H}_{l2}}{T_{WC}} \tag{5. 8}$$

- Dynamics of the surge tank:

$$\frac{d\overline{H}_r}{dt} = \frac{\overline{U}_c - \overline{U}_t}{C_s} \tag{5. 9}$$

The equations of the nonlinear model of a hydraulic turbine, presented above, show strong nonlinearities of the system and the dependence of its behaviour on the operating point. The equations of the model *with no* surge tank effects are (5. 1) to (5. 6), some of these equations correspond to model WG2 and the others are taken from Kundur (1994); on the other hand the equations (5. 1) to (5. 9) represent the model *with* surge tank effects, many of these equations correspond to model WG4 and the others are taken from Kundur(1994). Both models consider the case of a hydraulic power plant supplying an isolated load.

5.3 Nonlinear Controllers for Hydraulic Turbines with no Surge Tank Effects

5.3.1 The Cost Functions

This subsection introduces two useful cost functions for the comparison studies.

5.3.1.1 The Cost Function A

It is necessary to define a cost function in order to design optimal controllers or compare different control algorithms. The first cost function has three terms and is represented by:

$$f_{cost(A)} = c_1 \cdot \int_{ti}^{tf} \left|\overline{\omega}_{ref} - \overline{\omega}_r\right| \cdot t \cdot dt + c_2 \cdot \int_{ti}^{tf} \left|\overline{G}_d - \overline{G}\right| \cdot t \cdot dt + c_3 \cdot \int_{ti}^{tf} \left|\frac{\partial \overline{G}}{\partial t}\right| \cdot t \cdot dt \quad (5.\ 10)$$

The first component corresponds to the integral of the absolute value of the difference between the speed reference and the measured rotor speed multiplied by the time. This term penalises the speed error, its duration and long periods of time. The second and the third components correspond to the control effort that takes into account the gate movement. These terms penalise those actions of the controller that can produce damage or undesirable collateral effects, such as water hammer or cavitation, physical wear or simply excessive work in the gate actuator. Thus, these two terms penalise the amplitude and the duration of the manoeuvres, mainly those that extend during long periods of time.

5.3.1.2 The Cost Function B

The cost function B has three terms also and is represented by:

$$f_{cost(B)} = c_1 \cdot \int_{ti}^{tf} \left|\overline{\omega}_{ref} - \overline{\omega}_r\right| \cdot dt + c_2 \cdot \int_{ti}^{tf} \left|\overline{G}_d - \overline{G}\right| \cdot dt + c_3 \cdot \int_{ti}^{tf} \left|\frac{\partial \overline{G}}{\partial t}\right| \cdot dt \quad (5.\ 11)$$

In this case the first term penalises the speed error and its duration, besides it is represented by the integral of the absolute value of the difference between the speed reference and the measured rotor speed. The second and the third terms penalise the controller actions that can produce damage, physical wear or excessive work in the gate actuator. These two terms only penalise the amplitude of the manoeuvres and its duration.

5.3.2 PID Controllers

Three classical controllers are presented in this subsection; these are the PID, the PI-PD, the Gain Scheduling PID and the Gain Scheduling PI-PD.

5.3.2.1 Fixed PID controllers

Figure 5.3 shows the standard PID controller of a hydraulic power plant (IEEE Working Group, 1992; Kundur, 1994).

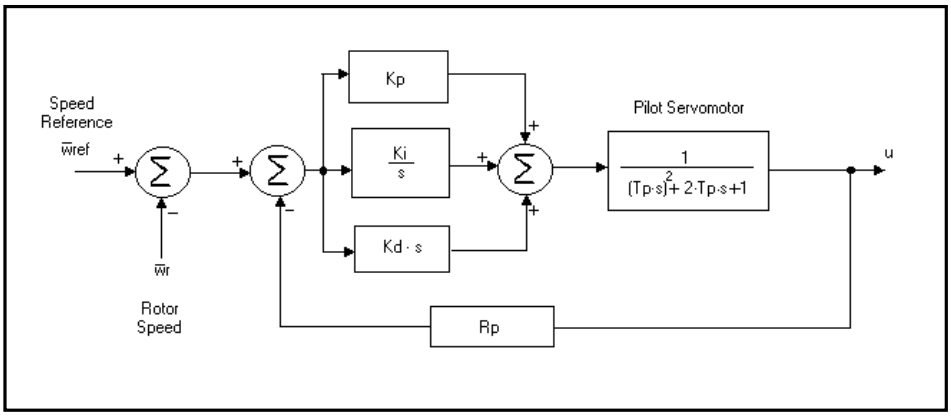

Figure 5.3: PID Controller.

5.3.2.2 PI-PD controller

Figure 5.4 depicts a PI-PD controller for a hydroelectric plant (Boireau, 1994).

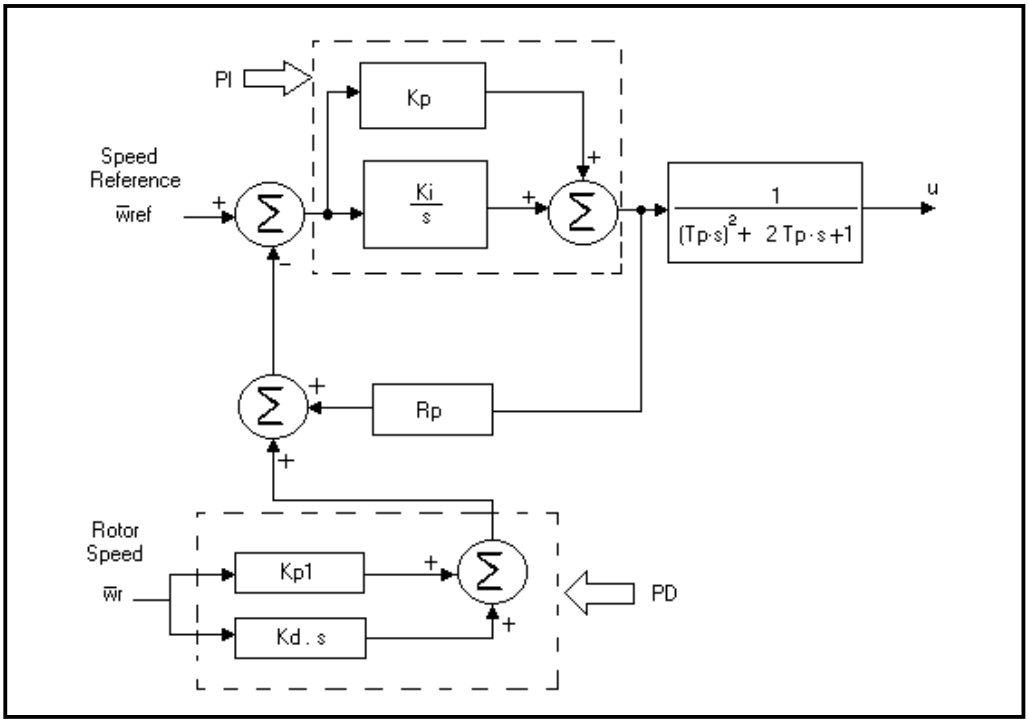

Figure 5.4: PI-PD Controller.

5.3.2.3 Gain Scheduling Controllers

The Gain Scheduling PID consists of a PID controller where the gains K_p, K_i and K_d are obtained by interpolating, or "scheduling", the optimised load values. On the other hand, the Gain Scheduling PI-PD is a PI-PD controller where the gains K_{p1}, K_p, K_i and K_d may be obtained by means of interpolation the optimised load values

5.3.3 Nonlinear Controllers

The design of nonlinear controllers using differential geometry techniques requires writing the equations of the hydraulic turbine model as a nonlinear system in the state space.

The partial state feedback linearization theorem (Marino and Tomei, 1995) guarantees that any nonlinear system $\dot{\mathbf{x}} = \mathbf{f}(\mathbf{x}) + \mathbf{g}(\mathbf{x}) \cdot u$ is locally partially state feedback linearizable with index r=1. According to this, there exists a local diffeomorphism $\mathbf{z} = \Phi(\mathbf{x})$ with $\Phi(\mathbf{0}) = \mathbf{0}$, where in **z**-coordinates the system becomes

$$\begin{pmatrix} \dot{z}_1 \\ \dot{z}_2 \end{pmatrix} = \begin{pmatrix} L_f \phi_1 \\ L_f \phi_2 + u) \end{pmatrix}$$

By utilising the feedback transformation $u = -L_f \phi_2 + v$; then,

$$\begin{pmatrix} \dot{z}_1 \\ \dot{z}_2 \end{pmatrix} = \begin{pmatrix} L_f \phi_1(\mathbf{z}) \\ v \end{pmatrix}$$

In the work of Quiroga, Batlle and Riera (2000), for the nonlinear model of the hydroelectric plants (with non-elastic water column and with no surge tank) the state variables of the system are $x_1 = \overline{U}_t$ and $x_2 = \overline{G} - \overline{G}_0$. Hence, the combination of equations (5. 1), (5. 2), (5. 3) and (5. 5) can be written together as a nonlinear system in $\mathbf{R}^2$

$$\mathbf{f}(\mathbf{x}) = \begin{pmatrix} \frac{1}{T_{WP}} \cdot \left(\overline{H}_0 - \left(f_p + \frac{1}{\left(x_2 + \overline{G}_0 \right)^2} \right) \cdot x_1^2 \right) \\ -\frac{x_2}{T_g} \end{pmatrix} \qquad (5.\ 12)$$

$$\mathbf{g}(\mathbf{x}) = \begin{pmatrix} 0 \\ 1/T_g \end{pmatrix} \qquad (5.\ 13)$$

The output of the system is x_2. The system $\dot{\mathbf{x}} = \mathbf{f}(\mathbf{x}) + \mathbf{g}(\mathbf{x}) \cdot u$ and $y = h(x_1, x_2) = x_2$ is said to have relative degree 'r' at a point $\mathbf{x}^0$ if:

1) $L_{\mathbf{g}} L_{\mathbf{f}}^{\,k} h(\mathbf{x}) = 0$ for all $\mathbf{x}$ in a neighbourhood of $\mathbf{x}^0$ and all $k < r - 1$.

2) $L_{\mathbf{g}} L_{\mathbf{f}}^{\,r-1} h(\mathbf{x}^0) \neq 0$.

To obtain the relative degree of the nonlinear system is necessary to compute

$$L_{\mathbf{g}} h(x_1^{\,0}, x_2^{\,0}) = \nabla h(x_1^{\,0}, x_2^{\,0}) \cdot \mathbf{g},$$

where $\left(x_1^{\,0}, x_2^{\,0}\right)$ is an equilibrium point. Computation yields

$$L_{\mathbf{g}} x_2 = \frac{1}{T_g} > 0$$

Therefore, in this case the relative degree is r = 1.

For this case the local diffeomorphism is

$$\begin{pmatrix} z_1 \\ z_2 \end{pmatrix} = \begin{pmatrix} \phi_1(\mathbf{x}) \\ \phi_2(\mathbf{x}) \end{pmatrix} = \begin{pmatrix} x_1 \\ T_g \cdot x_2 \end{pmatrix}$$

Therefore, the control effort is given by

$$u = -L_f \phi_2 + v = x_2 + v \qquad (5.\ 14)$$

Once the plant is partially state feedback linearized, the control is exerted by an outer loop with a PI or PI-PD controller. The resulting system is thus a "mixed" nonlinear control system. Two different controllers can be designed differing in the PI or PI-PD structure.

Figure 5.5 presents a first design by using partial state feedback linearization and a PI structure. This controller is called NL A.

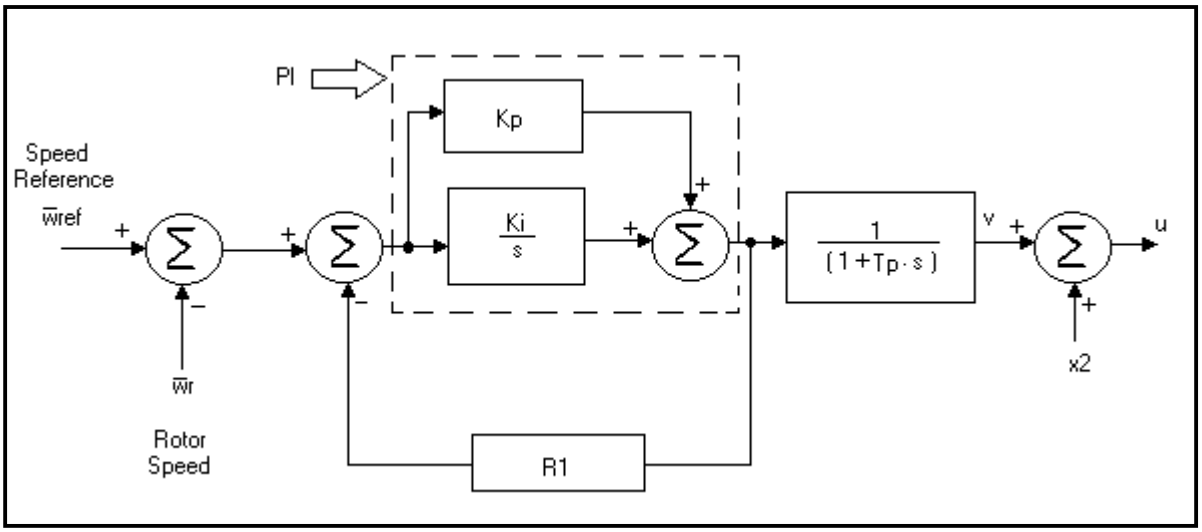

Figure 5.5: Nonlinear Controller A (NL A).

A second design is presented in Figure 5.6; a different structure (PI-PD) is considered and is called NL B. Both controllers (NL A and NL B) can be used in the general speed control scheme of Figure 5.7.

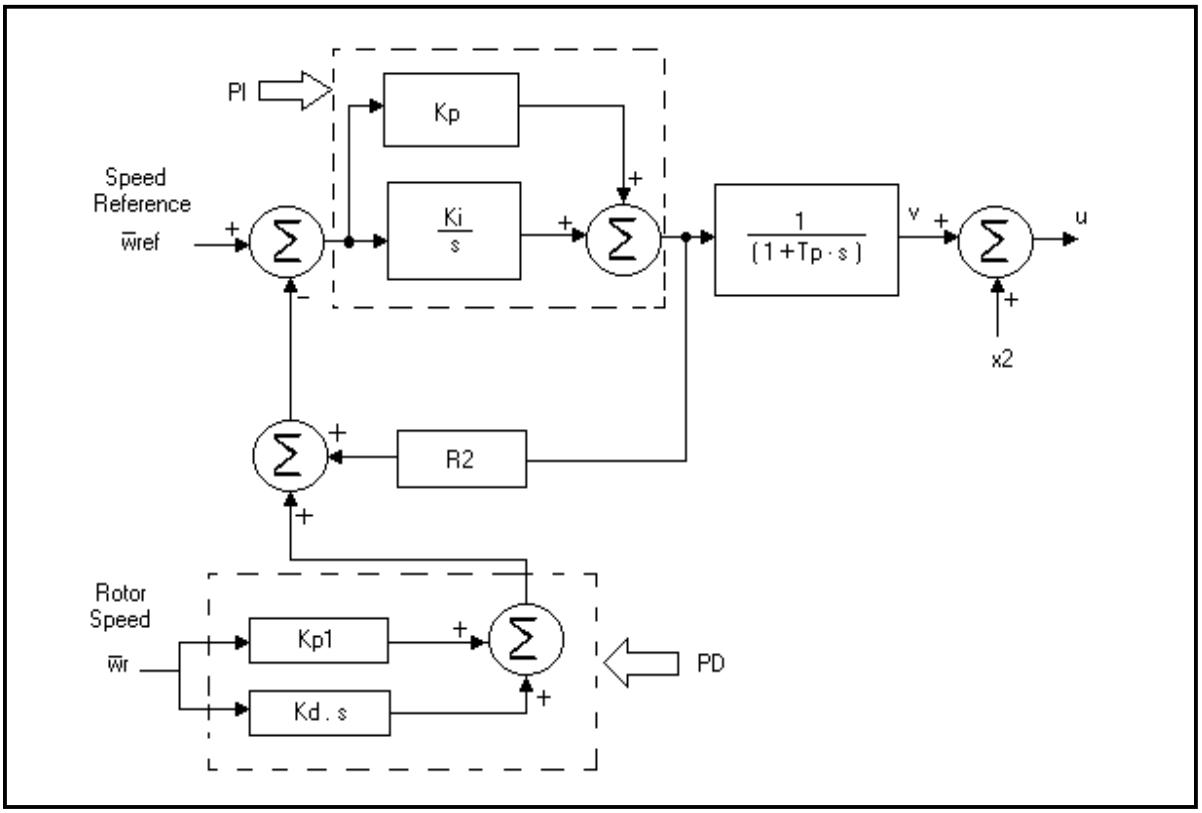

Figure 5.6: Nonlinear Controller B (NL B).

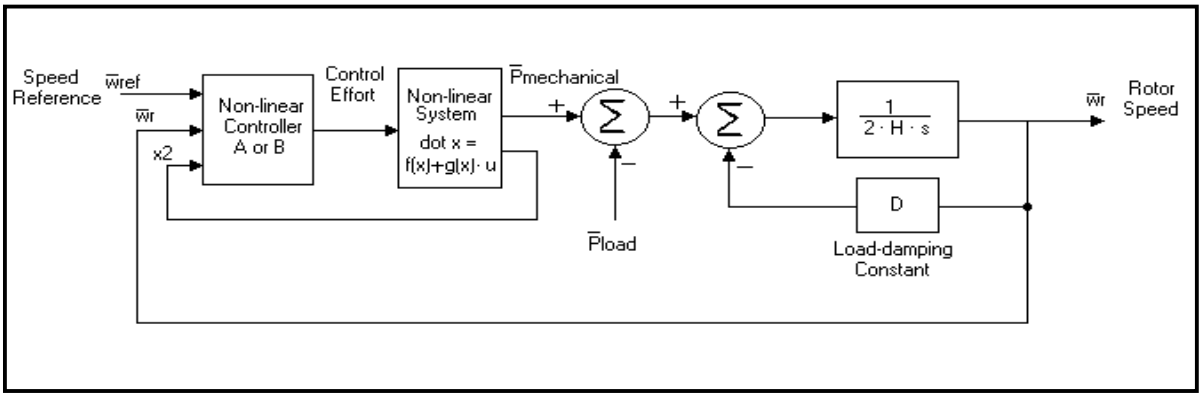

Figure 5.7: General speed control scheme for the controllers NL A or NL B.

The dynamics of a nonlinear system is decomposed, by means of partial state feedback linearization or input-output linearization, into an external part, which is a linear relation between the input and the output, and an internal part (no observable). In the next Subsection a study of this internal part is introduced.

5.3.4 The Zero Dynamics of the Nonlinear System with no Surge Tank Effects

The zero dynamics corresponds to the dynamics which describes the internal behaviour of the nonlinear system when the input and the initial conditions have been chosen in a way to keep the output to remain identically zero. Moreover, the zero dynamics allows to draw some conclusions about the stability of the internal dynamics.

Hence, taking x_2=0, the vectorial field of the zero dynamics is given by:

$$\tilde{f}(x_1) = \frac{1}{T_{WP}} \cdot \left(\overline{H}_0 - (f_p + \frac{1}{\overline{G}_0^{\,2}}) \cdot x_1^{\,2} \right)$$

This is cancelled out, taken only the positive solution, in:

$$x_1^{\,*} = \sqrt{\frac{\overline{H}_0}{f_p + \frac{1}{\overline{G}_0^{\,2}}}}$$

and

$$\tilde{f}'(x_1^*) = -\frac{2}{T_{WP}} \cdot \left(f_p + \frac{1}{\overline{G}_0^{\,2}} \right) \cdot x_1^* = -\frac{2}{T_{WP}} \cdot \sqrt{f_p + \frac{1}{\overline{G}_0^{\,2}}} \cdot \sqrt{\overline{H}_0} < 0$$

Therefore, the zero dynamics is linearly asymptotically stable. Moreover, is globally stable since:

when $x_1 > x_1^*$, $\tilde{f}(x_1) < 0$ then x_1 decreases to x_1^*.

when $x_1 < x_1^*$, $\tilde{f}(x_1) > 0$ then x_1 increases to x_1^*.

5.3.5 Comparative Studies Using $f_{cost(A)}$

This subsection presents comparative studies of the behaviour of six different controllers: PID, Gain Scheduling PID, PI-PD, Gain Scheduling PI-PD, NL A and NL B. Quiroga, Batlle and Riera (2000) present comparative studies only for the PID, Gain Scheduling PID, NL A and NL B controllers. In this subsection those comparative studies are extended by including the PI-PD and the Gain Scheduling PI-PD controllers. The studies are done for different operating points defined by the disturbance $\overline{P}_{load}$ (non-frequency-sensitive load).

The first study is equivalent to the comparison of the rotor speed response to different load changes. The second study corresponds to a comparison of the cost function values. The values of the weight coefficients of the cost function (5. 10) are chosen according to practical experience in hydroelectric plants (Riera and Cardoner, 1992) and correspond to the following values c_1=0.6, c_2=0.2 and c_3=0.2. These studies verify the constraints of maximum gate opening rate and maximum gate closing rate for all controllers. Typical values for these constraints are 0.16 [pu/s] (Kundur, 1994).

The parameters of the PID, PI-PD, NL A and NL B controllers are adjusted according to the minimal value of the cost function after applying a step function on the disturbance $\overline{P}_{load}$ from 0.8 [pu] to 0.9 [pu]. This operating point corresponds to the worst case for controllers with fixed parameters.

Table 5.1 shows the values of the parameters of the controllers PID, PI-PD, NL A and NL B obtained after this adjustment. The meanings of the parameters of the controllers are shown in Table 5.2. In these studies the parameters from St. Lawrence power plant are used (i.e. the Parameters 5, Table 3.5 Chapter 3).

Controller	K_p	K_i	K_d	K_{p1}	R_p	R_1	R_2	$f_{cost(A)}$
PID	3	0.6	2	-	0	-	-	0.3505
PI-PD	0.5	0.7	4	1	0	-	-	0.3188
NL A	5	20	-	-	-	10	-	45.250
NL B	1.5	0.3	5	1	-	-	2.5	0.2590

Table 5. 1: Parameters of PID, PI-PD, NL A and NL B controllers.

Parameters	Meanings
$K_{p,p1,i,d}$	Gains of a PID, PI-PD in [pu] (p and p1: proportional, i: integral, d: derivative)
R_p	Temporary droop in [pu].
$R_{1,2,3,4}$	Feedback gains in [pu].
$c_{1,2,3}$	Weight coefficients of the cost functions in [pu].

Table 5. 2: Meanings of the parameters of the controllers.

The parameters of the Gain Scheduling PID and the Gain Scheduling PI-PD are adjusted for each operating point according to the minimal value of the cost function after applying a 0.1 step function on the disturbance $\overline{P}_{load}$. Table 5.3 shows for each operating point the values of the parameters of these controllers.

Controllers	**Gain Scheduling PID**				**Gain Scheduling PI-PD** (K_{p1}=1)			
Operating Points	K_p	K_i	K_d	$f_{cost(A)}$	K_p	K_i	K_d	$f_{cost(A)}$
$\overline{P}_{load}$: from 0.8 to 0.9	3.0	0.6	1.5	0.3505	0.5	0.7	4	0.3188
$\overline{P}_{load}$: from 0.7 to 0.8	2.8	0.6	1.5	0.3318	0.51	0.71	3.95	0.2985
$\overline{P}_{load}$: from 0.6 to 0.7	2.7	0.6	1.6	0.3210	0.53	0.71	3.91	0.2843
$\overline{P}_{load}$: from 0.5 to 0.6	2.6	0.6	1.7	0.3140	0.52	0.72	3.97	0.2791
$\overline{P}_{load}$: from 0.4 to 0.5	2.7	0.6	1.8	0.3130	0.51	0.72	3.95	0.2730
$\overline{P}_{load}$: from 0.3 to 0.4	2.7	0.6	1.9	0.3110	0.53	0.75	4.1	0.2702
$\overline{P}_{load}$: from 0.2 to 0.3	2.7	0.6	1.9	0.3071	0.5	0.71	4	0.2690
$\overline{P}_{load}$: from 0.1 to 0.2	2.6	0.6	1.8	0.3020	0.55	0.72	4	0.2655
$\overline{P}_{load}$: from 0.0 to 0.1	2.6	0.65	2.0	0.2970	0.58	0.75	4.1	0.2605

Table 5. 3: Values of the parameters for the Gain Scheduling PID and the Gain Scheduling PI-PD ($f_{cost(A)}$).

5.3.5.1 Comparison of Rotor Speed Behaviour for Different Load Changes

Figures 5.8 to 5.13 show the rotor speed response for three different loads.

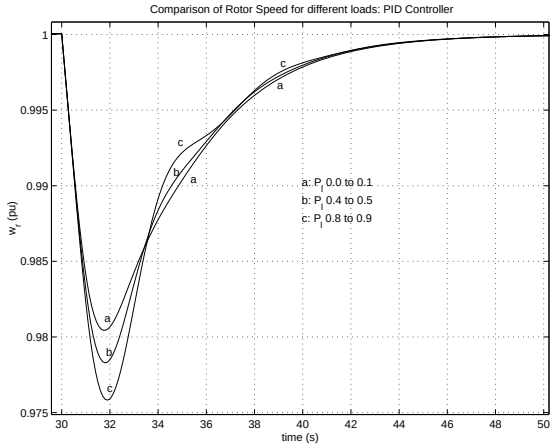

Figure 5.8: Comparison of rotor speed.

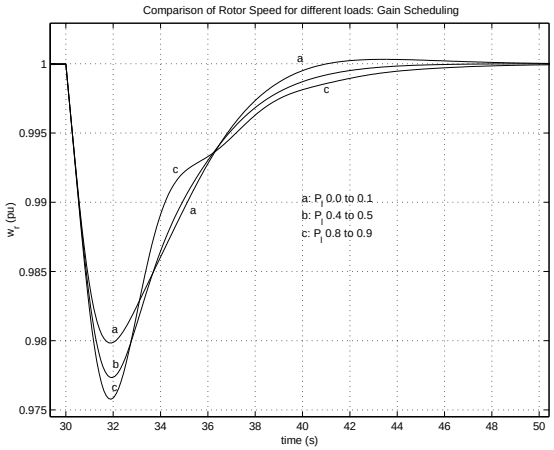

Figure 5.9: Comparison of rotor speed.

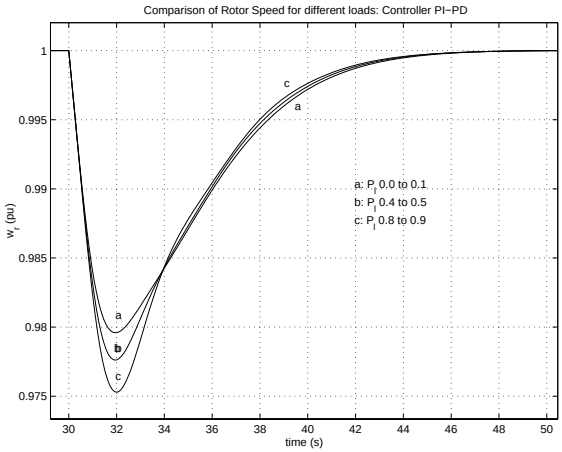

Figure 5.10: Comparison of rotor speed.

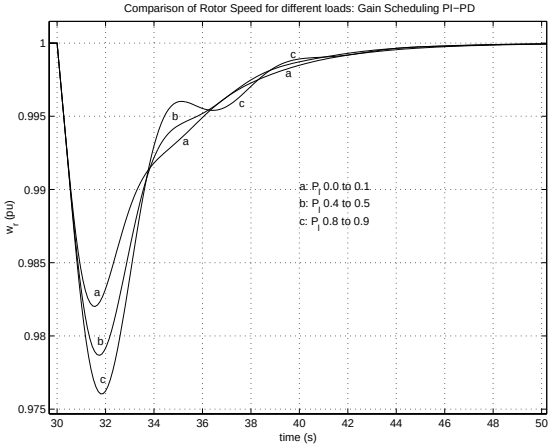

Figure 5.11: Comparison of rotor speed.

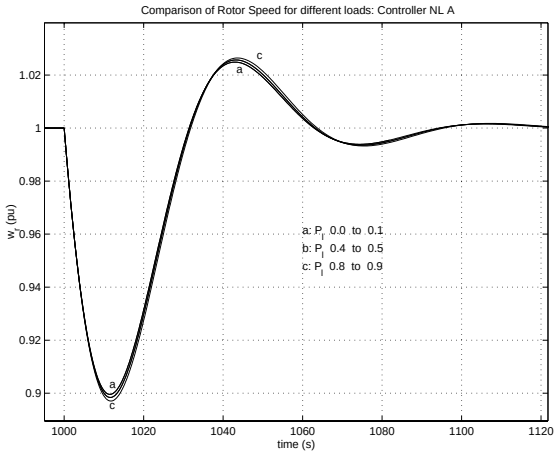

Figure 5.12: Comparison of rotor speed.

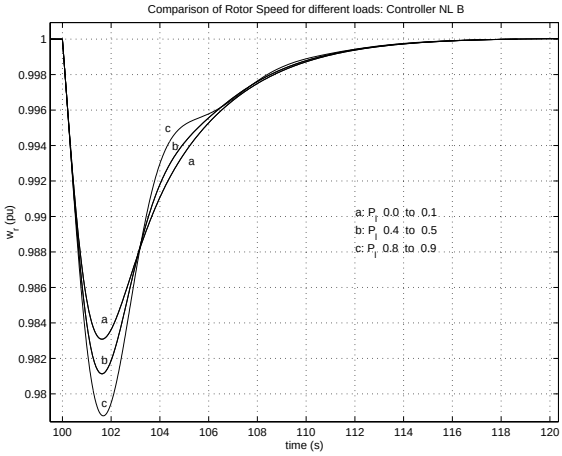

Figure 5.13: Comparison of rotor speed.

Responses of the rotor speed for the Controller NL A are very poor since the system reaches the steady state value after a time period three times greater than the remaining cases. Hence, this fact is reflected and penalised with large values of the cost function. Controller NL B, on the other hand, presents a satisfactory behaviour. Moreover, the cost function takes the lowest value for each operating point.

5.3.5.2 Comparison of Cost Function Values ($f_{cost(A)}$)

Figure 5.14 shows the values of the cost function for the controllers PID, PI-PD, Gain Scheduling PID, Gain Scheduling PI-PD and NL B for discrete operating points, which are joined by straight lines.

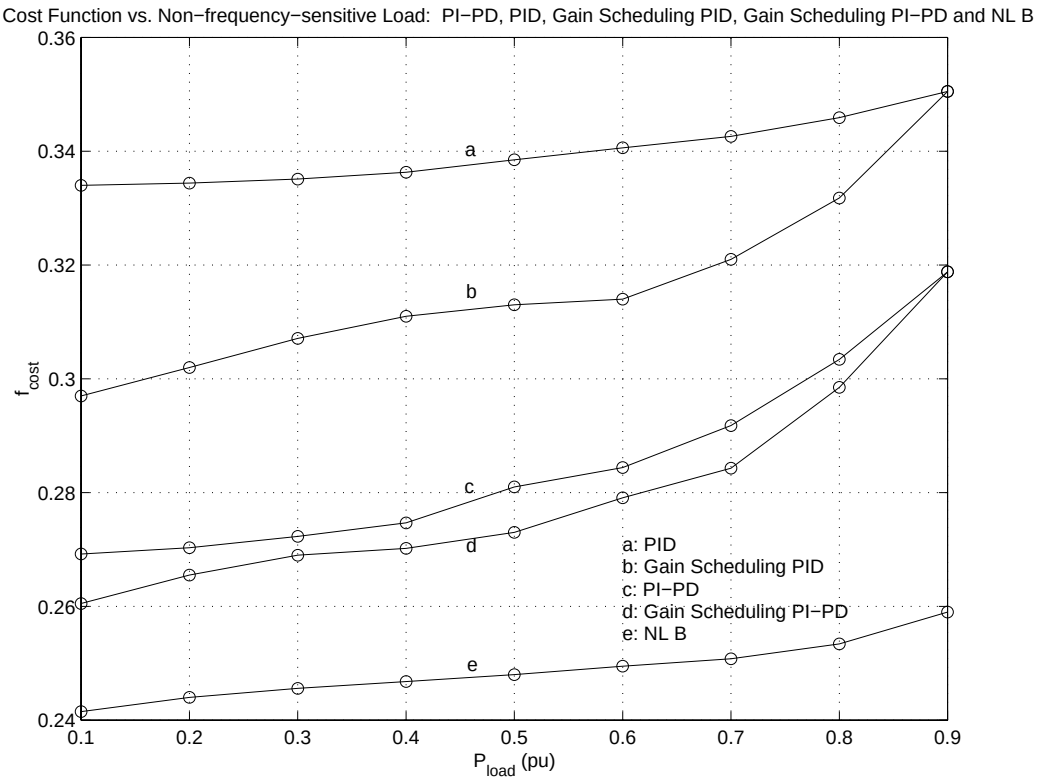

Figure 5.14: Comparison of cost function values ($f_{cost(A)}$).

Since the parameters of the controllers are optimised at the operating point 0.9 [pu], the cost function value (0.3188) of the PI-PD coincides with the value of the Gain Scheduling PI-PD. For the remaining operating points the values of the cost function of the PI-PD controller are greater than the values for the Gain Scheduling PI-PD since the parameters of the later are optimised for each operating point.

Cost function values in the case of the controller NL B are the lowest for all operating points. For the controller NL B these values are between 11 and 19 per cent lower than the Gain Scheduling PI-PD case. This means that the controller NL B produces a good dynamic behaviour with a reduced wear in the gate servos. Thus, by using this controller, the hydroelectric system obtains the most homogeneous response of the rotor speed.

5.3.6 Controller Adjustment Surfaces Using $f_{cost(A)}$

In this subsection fine adjustments for two controllers are presented. The 3-D graphics show a level surface where the minimum is found. The discrete points of the 3-D graphics are

obtained by adjusting the parameters of the controller according to the minimal value of the cost function after applying a step function on the disturbance $\overline{P}_{load}$ from 0.8 [pu] to 0.9 [pu].

5.3.6.1 Adjustment for the PI-PD Controller

This case represents the level surface $f_{cost(A)} = f(K_p, K_i)$, with $K_d = 4$. For values of K_d greater or lower than 4 one obtains other surfaces whose values are greater (for each pair K_p and K_i) than the values represented in Figure 5.15.

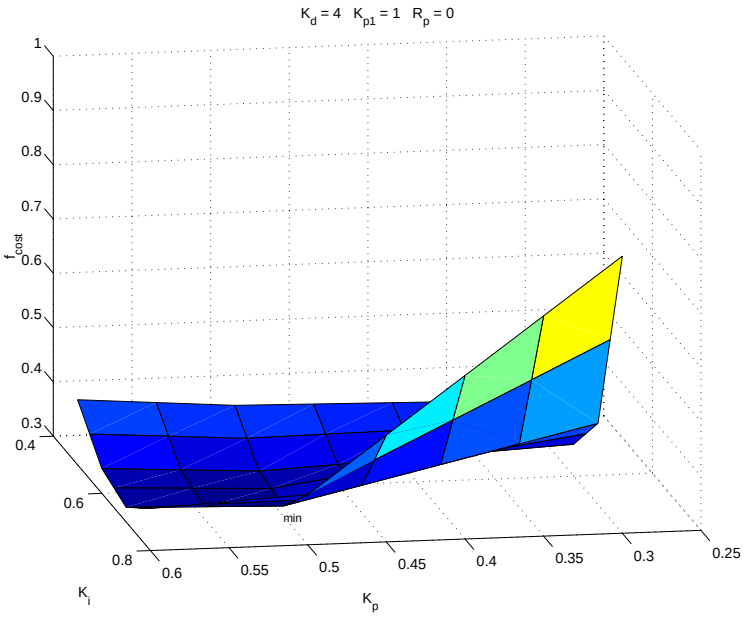

Figure 5.15: Adjustment surface for the PI-PD controller ($f_{cost(A)}$).

Figures 5.16 and 5.17 show transversal cuts with different planes.

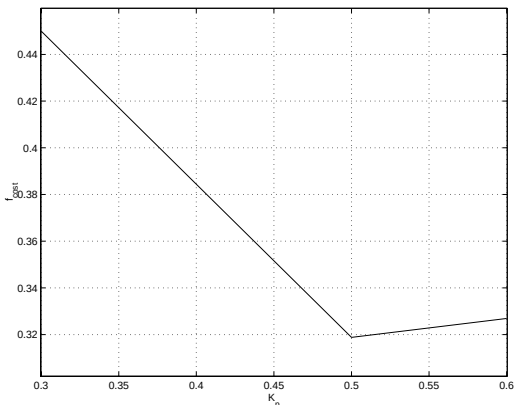

Figure 5.16: Plane $K_i = 0.7$.

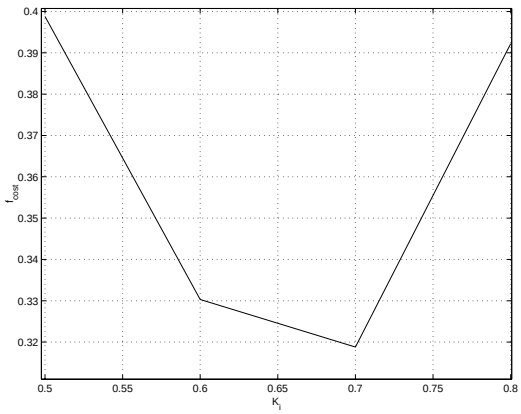

Figure 5.17: Plane $K_p = 0.5$.

5.3.6.2 Adjustment for the Nonlinear Controller NL B

This controller is based on the PI-PD structure; therefore, its cost function is $f_{cost(A)} = f(K_p, K_i, K_d)$. In Figure 5.18 a level surface of $f_{cost(A)} = f(K_p, K_i)$ with $K_d = 5$ is depicted.

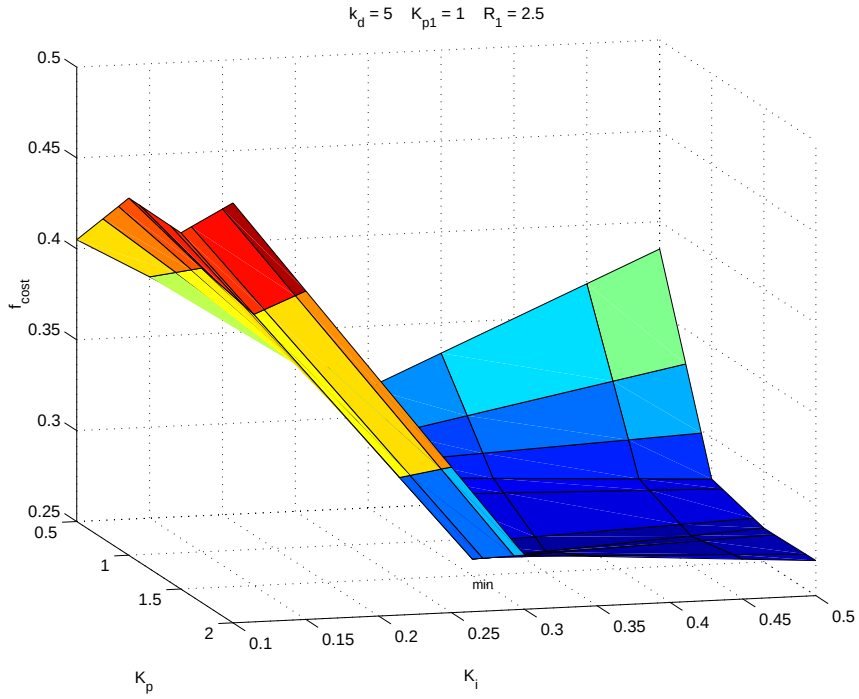

Figure 5.18: Adjustment surface for the controller NL B ($f_{cost(A)}$).

Figures 5.19 and 5.20 present transversal cuts with different planes in order to show the minimal value.

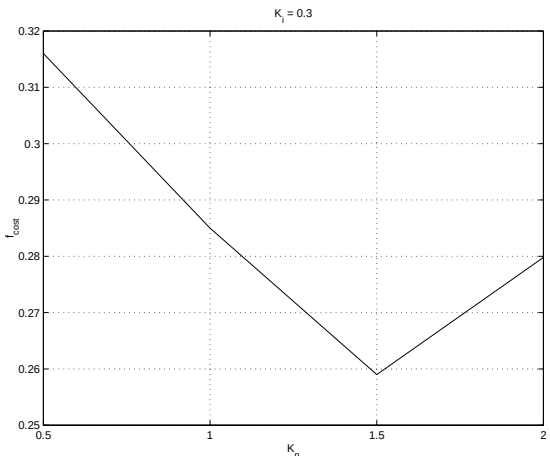

Figure 5.19: Plane $K_i = 0.3$

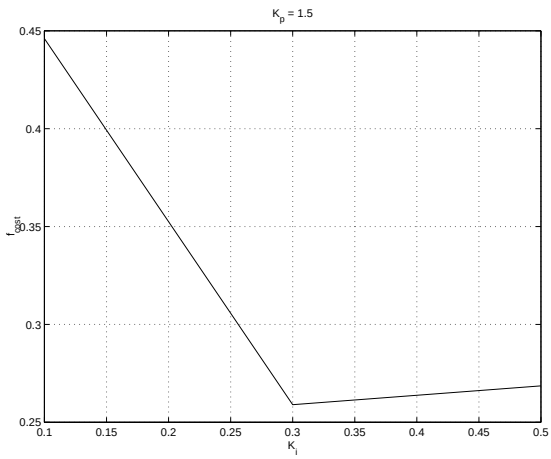

Figure 5.20: Plane $K_p = 1.5$

5.3.7 Comparative Studies Using $f_{cost(B)}$

This subsection presents comparative studies of the behaviour of six different controllers: PID, PI-PD, Gain Scheduling PID, Gain Scheduling PI-PD, NL A and NL B. The chosen cost function is $f_{cost(B)}$. The studies are also done for different operating points defined by the non-frequency-sensitive load $\overline{P}_{load}$.

The main study corresponds to a comparison of the cost function values. Again, the values of the weight coefficients of the cost function, $f_{cost(B)}$ given by equation (5. 11), are chosen according to practical experience in hydroelectric plants (Riera and Cardoner, 1992) and correspond to the well known values c_1=0.6, c_2=0.2 and c_3=0.2.

The parameters of the PID, PI-PD, NL A and NL B controllers are adjusted according to the minimal value of the cost function after applying a step function on the disturbance $\overline{P}_{load}$ from 0.8 [pu] to 0.9 [pu]. Table 5.4 shows the values of the parameters of the controllers PID, PI-PD, NL A and NL B obtained after this adjustment.

Controller	K_p	K_i	K_d	K_{p1}	R_p	R_1	R_2	$f_{cost(B)}$
PID	2.75	0.7	1.75	-	0	-	-	0.1020
PI-PD	0.5	0.6	4	1	0	-	-	0.1069
NL A	5	20	-	-	-	10	-	1.3170
NL B	1.5	0.3	5	1	-	-	2.5	0.09092

Table 5.4: Parameters of PID, PI-PD, NL A and NL B controllers.

Table 5.5 presents the values of the parameters of the Gain Scheduling PID and Gain Scheduling PI-PD for each operating point.

Controllers	**Gain Scheduling PID**				**Gain Scheduling PI-PD** (K_{p1}=1)			
Operating Points	K_p	K_i	K_d	$f_{cost(B)}$	K_p	K_i	K_d	$f_{cost(B)}$
$\overline{P}_{load}$: from 0.8 to 0.9	2.75	0.7	1.75	0.1020	0.5	0.6	4	0.1069
$\overline{P}_{load}$: from 0.7 to 0.8	2.7	0.7	1.8	0.0998	0.53	0.63	4.1	0.1040
$\overline{P}_{load}$: from 0.6 to 0.7	2.8	0.7	1.8	0.0976	0.55	0.67	4.1	0.1010
$\overline{P}_{load}$: from 0.5 to 0.6	2.9	0.7	1.9	0.0957	0.52	0.68	4.2	0.0989
$\overline{P}_{load}$: from 0.4 to 0.5	2.8	0.7	2.0	0.0941	0.6	0.67	4.1	0.0963
$\overline{P}_{load}$: from 0.3 to 0.4	2.8	0.7	2.1	0.0928	0.5	0.66	4.2	0.0948
$\overline{P}_{load}$: from 0.2 to 0.3	3.0	0.7	2.1	0.0906	0.5	0.66	4.3	0.0931
$\overline{P}_{load}$: from 0.1 to 0.2	3.1	0.7	2.1	0.0894	0.6	0.67	4.2	0.0916
$\overline{P}_{load}$: from 0.0 to 0.1	3.1	0.7	2.0	0.0881	0.5	0.65	4.1	0.0900

Table 5.5: Parameter values of the Gain Scheduling PID and Gain Scheduling PI-PD ($f_{cost(B)}$).

5.3.7.1 Comparison of Cost Function Values ($f_{cost(B)}$)

Figure 5.21 shows the values of the cost function ($f_{cost(B)}$) for the controllers PID, PI-PD, Gain Scheduling PID, Gain Scheduling PI-PD and NL B for discrete operating points, which are joined by straight lines.

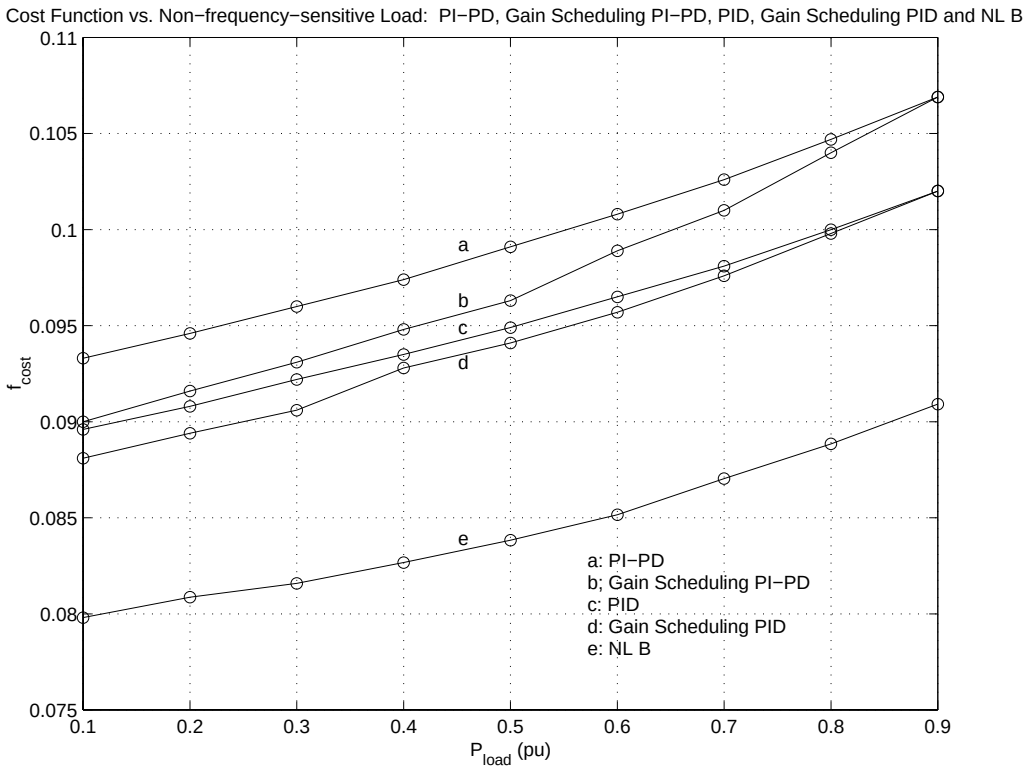

Figure 5.21: Comparison of cost function ($f_{cost(B)}$).

For many operating points the values of the cost function of the PID controller are greater than the values for the Gain Scheduling PID since the parameters of this controller are optimised for each operating point. Only for the 0.9 [pu] load they coincide, since the parameters of both controllers are optimised in that operating point.

Cost function values in the case of the controller NL B are the lowest for all operating points. Values for the controller NL B are between 10 and 13 per cent lower than the values of the Gain Scheduling PID. Once again, the controller NL B produces a good dynamic behaviour with reduced wear in the gate servos.

5.3.8 Controllers Adjustment Surfaces Using $f_{cost(B)}$

5.3.8.1 Adjustment for the PID Controller

For the case of the PID controller the 3-D graphic represents a level surface, where $f_{cost(B)} = f(K_p, K_d)$ and $K_i = 0.7$. For others values of K_i greater or lower than 0.7 other

surfaces are obtained, whose values are greater (for each pair K_p and K_d) than the values represented in Figure 5.22.

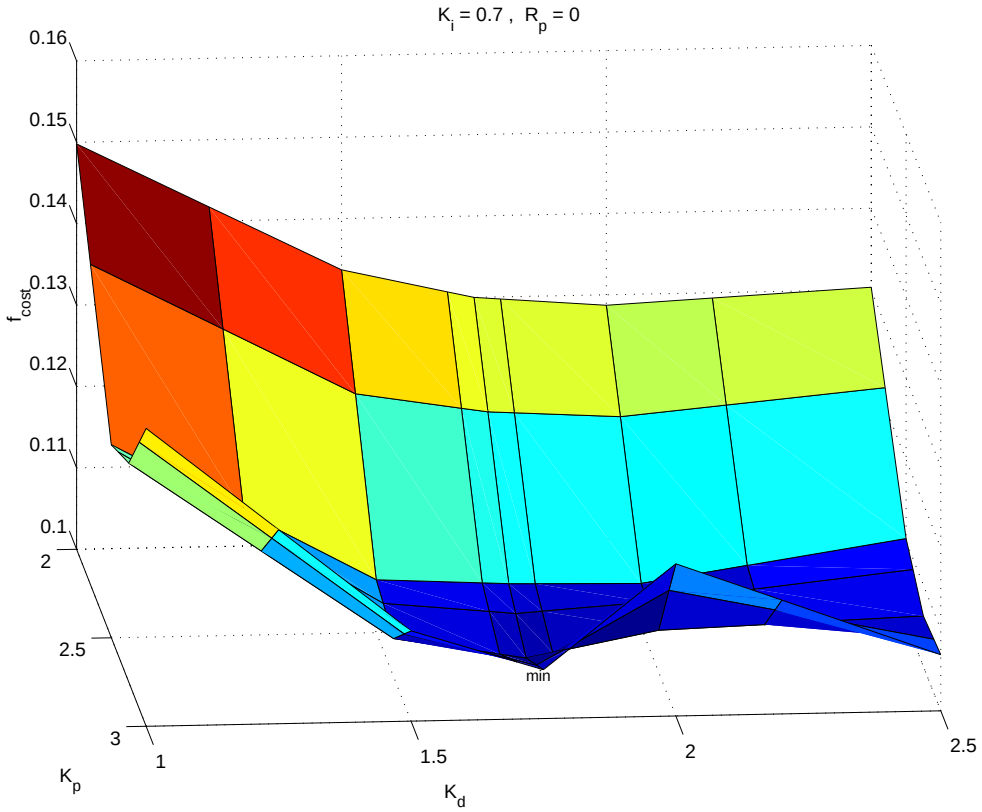

Figure 5.22: Adjustment surface for the PID controller ($f_{cost(B)}$).

Figures 5.23 and 5.24 present transversal cuts in order to show the minimal value for K_p and K_d.

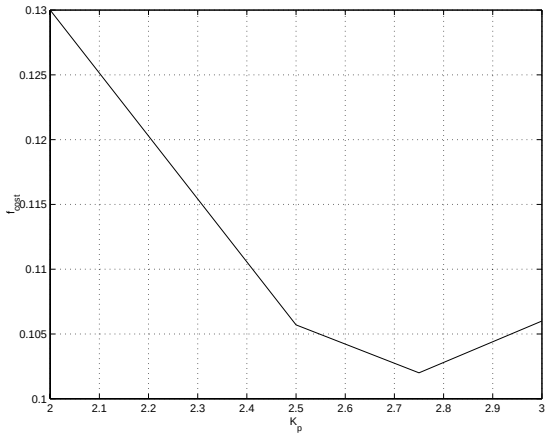

Figure 5.23: Plane K_d = 1.75.

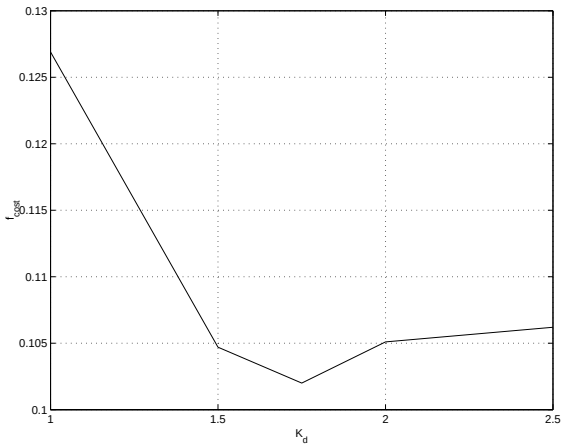

Figure 5.24: Plane K_p = 2.75.

5.3.8.2 Adjustment for the Nonlinear Controller NL B

This controller is based on the PI-PD structure; therefore, its cost function may be written as $f_{cost(B)} = f(K_p, K_i, K_d)$. In Figure 5.25 a level surface of $f_{cost(B)} = f(K_p, K_i)$ with $K_d = 5$ is depicted.

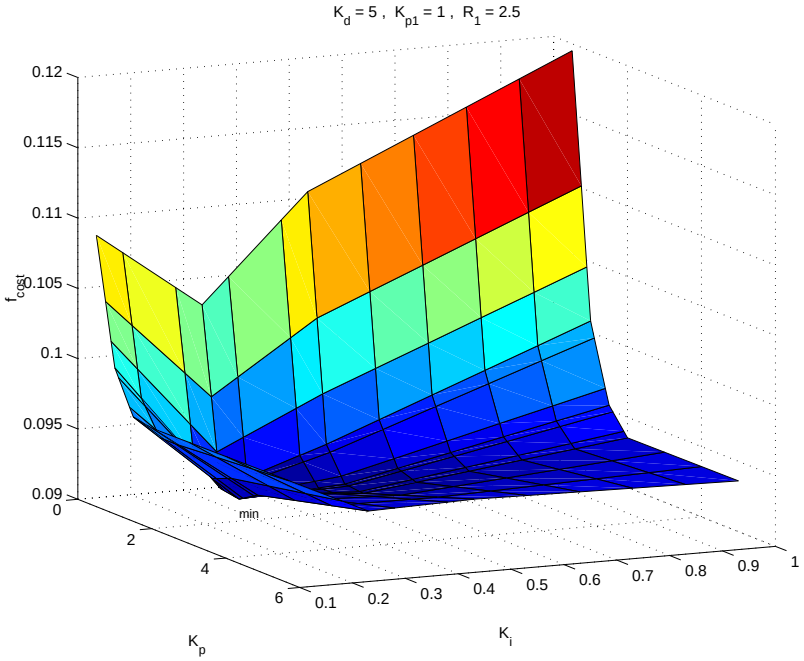

Figure 5.25: Adjustment surface for the controller NL B ($f_{cost(B)}$).

Figures 5.26 and 5.27 present transversal cuts with different planes in order to show the minimal value.

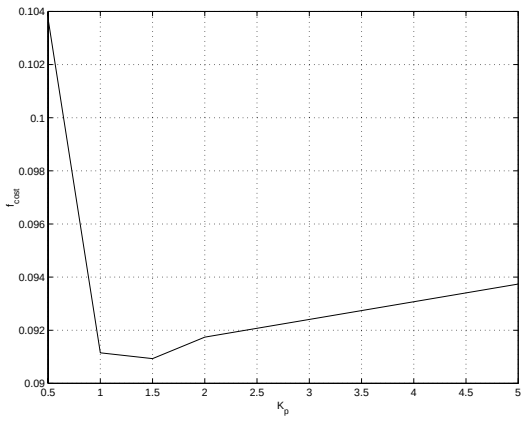

Figure 5.26: Plane $K_i = 0.3$

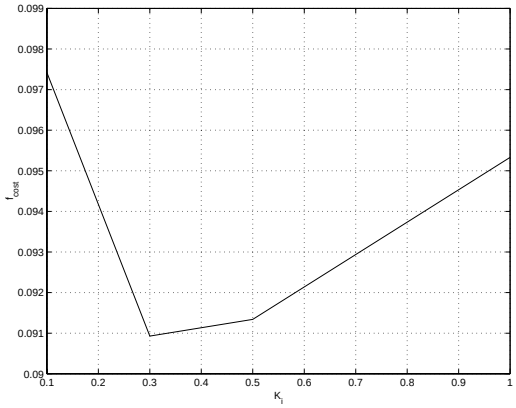

Figure 5.27: Plane $K_p = 1.5$

5.4 Nonlinear Controllers for Hydraulic Turbines with Surge Tank Effects

Sometimes, the design or tuning of the speed controller for a hydraulic plant with surge tank neglects the dynamics of the tunnel and the surge tank by considering a surge tank with infinite dimensions.

According to the conclusions obtained in Chapter 4 regarding the identification of a hydroelectric power plant with a surge tank, it is important to consider, in the design of the controllers, the dynamics of the tunnel and the surge tank. Moreover, Kundur (1994) points out the importance of long-term dynamic studies and also a long-term stability study.

This long-term stability study is associated with the response of a power system to severe upsets such as the disturbances that result in excursion of frequency (or voltage) either so great or so long-lasting that they involve the action of slow processes not modelled in conventional transient studies.

This subsection proposes the design of nonlinear controllers from nonlinear models of hydroelectric power plants when all the dynamics described in Section 5.2 are considered, including the dynamics of the tunnel and the surge tank. Indirectly, the long-term dynamic study is taken into account by checking the long-term stability.

5.4.1 Nonlinear Controllers

Once again, the partial state feedback linearization theorem guarantees that any nonlinear system $\dot{\mathbf{x}} = \mathbf{f}(\mathbf{x}) + \mathbf{g}(\mathbf{x}) \cdot \mathrm{u}$ is locally partially state feedback linearizable with index r=1. According to this, there exists a local diffeomorphism $\mathbf{z} = \Phi(\mathbf{x})$ with $\Phi(\mathbf{0}) = \mathbf{0}$, where in $\mathbf{z}$-coordinates the system becomes

$$\begin{pmatrix} \dot{z}_1 \\ \dot{z}_2 \\ \dot{z}_3 \\ \dot{z}_4 \end{pmatrix} = \begin{pmatrix} L_f \phi_1 \\ L_f \phi_2 \\ L_f \phi_3 \\ L_f \phi_4 + u \end{pmatrix}$$

By utilising the feedback transformation $u = -L_f \phi_4 + v$; then,

$$\begin{pmatrix} \dot{z}_1 \\ \dot{z}_2 \\ \dot{z}_3 \\ \dot{z}_4 \end{pmatrix} = \begin{pmatrix} L_f \phi_1 \\ L_f \phi_2 \\ L_f \phi_3 \\ v \end{pmatrix}$$

Putting together the different equations a nonlinear model in state space form may be obtained. In the case of a hydroelectric plant with non-elastic water columns, the state variables of the nonlinear system are $x_1 = \overline{U}_t$, $x_2 = \overline{H}_r$, $x_3 = \overline{U}_c$ and $x_4 = \overline{G} - \overline{G}_0$.

For the first equation of the nonlinear system it is necessary to combine equations (5. 1), (5. 2) and (5. 3). For the second and the fourth equations, (5. 9) and (5. 5) are used respectively. For the third equation of the nonlinear system (5. 7) and (5. 8) are combined. Thus, a nonlinear system in $\mathbf{R^4}$ is obtained and is represented as

$$\mathbf{f}(\mathbf{x}) = \begin{pmatrix} \frac{1}{T_{WP}} \cdot \left(x_2 - \left(f_p + \frac{1}{\left(x_4 + \overline{G}_0\right)^2} \right) \cdot x_1^2 \right) \\ \frac{x_3 - x_1}{C_s} \\ \frac{1}{T_{WC}} \cdot \left(\overline{H}_0 - x_2 - f_{p2} \cdot x_3 \cdot |x_3| \right) \\ -\frac{x_4}{T_g} \end{pmatrix} \tag{5. 15}$$

$$\mathbf{g}(\mathbf{x}) = \begin{pmatrix} 0 \\ 0 \\ 0 \\ 1/T_g \end{pmatrix} \tag{5. 16}$$

The output of the nonlinear system is x_4. The system $\dot{\mathbf{x}} = \mathbf{f}(\mathbf{x}) + \mathbf{g}(\mathbf{x}) \cdot u$ and $y = h(x_1, x_2, x_3, x_4) = x_4$ is said to have relative degree ‘r’ at a point $\mathbf{x}^0$ if:

1) $L_{\mathbf{g}} L_{\mathbf{f}}{}^k h(\mathbf{x}) = 0$ for all $\mathbf{x}$ in a neighbourhood of $\mathbf{x}^0$ and all $k < r - 1$.

2) $L_{\mathbf{g}} L_{\mathbf{f}}{}^{r-1} h(\mathbf{x}^0) \neq 0$.

To obtain the relative degree of the nonlinear system is necessary to compute

$$L_{\mathbf{g}} h(x_1{}^0, x_2{}^0, x_3{}^0, x_4{}^0) = \nabla h(x_1{}^0, x_2{}^0, x_3{}^0, x_4{}^0) \cdot \mathbf{g},$$

where $\left(x_1^{\,0}, x_2^{\,0}, x_3^{\,0}, x_4^{\,0}\right)$ is an equilibrium point. Computation yields

$$L_g x_4 = \frac{1}{T_g} > 0$$

Therefore, also in this case, the relative degree is r = 1.

For this case the local diffeomorphism is

$$\begin{pmatrix} z_1 \\ z_2 \\ z_3 \\ z_4 \end{pmatrix} = \begin{pmatrix} \phi_1(\mathbf{x}) \\ \phi_2(\mathbf{x}) \\ \phi_3(\mathbf{x}) \\ \phi_4(\mathbf{x}) \end{pmatrix} = \begin{pmatrix} x_1 \\ x_2 \\ x_3 \\ T_g \cdot x_4 \end{pmatrix}$$

Therefore, for this case the control effort is

$$u = -L_f \phi_4 + v = x_4 + v \qquad (5.\ 17)$$

Two different controllers may be designed differing in the PI or PI-PD structure. Figure 5.28 presents a design by using partial state feedback linearization and the PI controller (controller NL C). Another design is presented in Figure 5.29 This controller is called NL D and is formed by a PI-PD structure and the partial state feedback linearization component. Both controllers can be applied in the general speed control scheme of Figure 5.30.

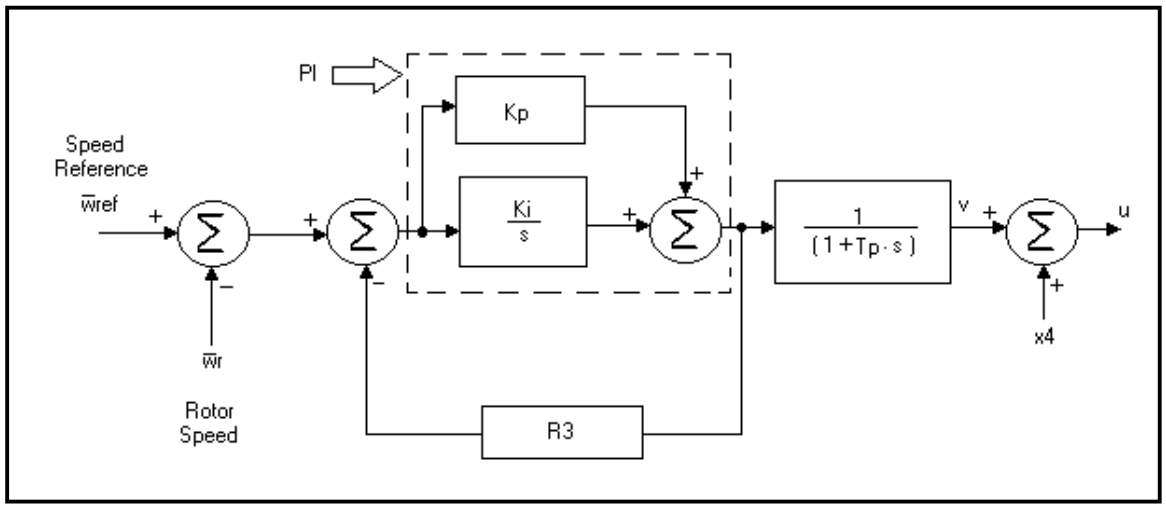

Figure 5.28: Nonlinear Controller C (NL C).

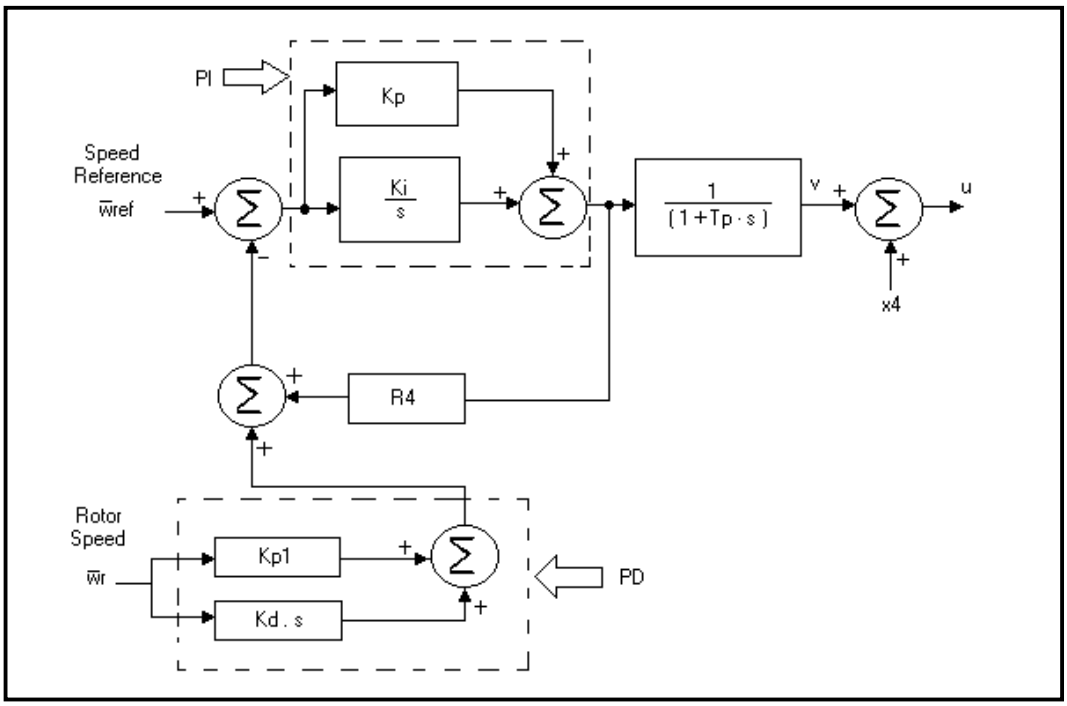

Figure 5.29: Nonlinear Controller D (NL D).

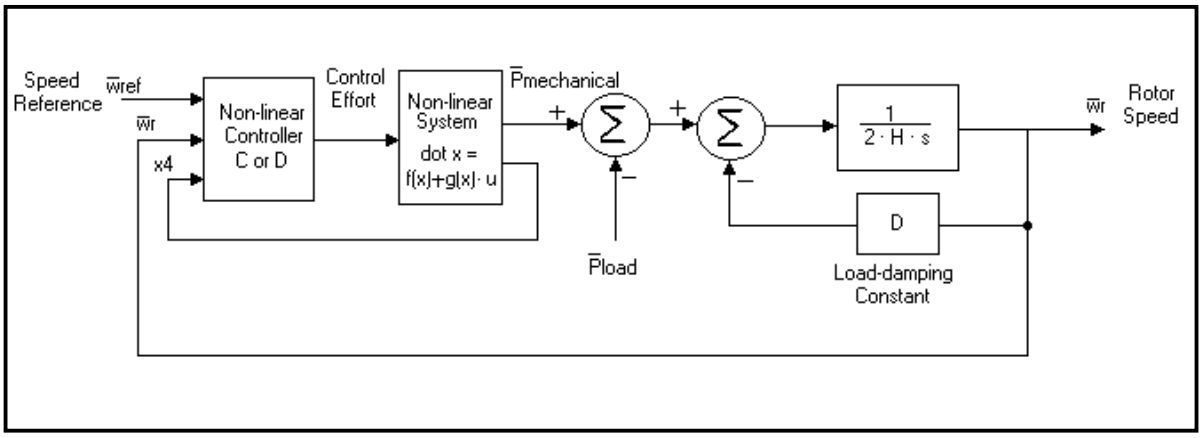

Figure 5.30: General speed control scheme for the controllers NL C or NL D.

5.4.2 The Zero Dynamics of the Nonlinear System with Surge Tank Effects

The study of the internal behaviour of the nonlinear system, given by (5. 15) and (5. 16), by means of the study of the zero dynamics is proposed. Recalling that the zero dynamics is defined to be the internal dynamics of this nonlinear system when the output of the nonlinear system is kept at zero by the input.

Hence, taking $x_4=0$, the vectorial field of the zero dynamics is given by:

$$\tilde{f}(x_1,x_2,x_3)=\begin{pmatrix}\frac{1}{T_{WP}}\cdot\left(x_2-(f_p+\frac{1}{\overline{G_0}^2})\cdot x_1^2\right)\\ \frac{x_3-x_1}{C_s}\\ \frac{1}{T_{WC}}\cdot\left(\overline{H}_0-x_2-f_{p2}\cdot x_3\cdot|x_3|\right)\end{pmatrix}$$

The equilibrium point is given by:

$$x_1^*=\sqrt{\frac{\overline{H}_0}{f_p+f_{p2}+\frac{1}{\overline{G_0}^2}}}$$

$$x_2^*=\left(f_p+\frac{1}{\overline{G_0}^2}\right)\cdot(x_1^*)^2$$

$$x_3^*=\sqrt{\frac{\overline{H}_0}{f_p+f_{p2}+\frac{1}{\overline{G_0}^2}}}=x_1^*$$

The jacobian of $\tilde{f}(x_1,x_2,x_3)$ in the equilibrium point (x_1^*,x_2^*,x_3^*) is:

$$\left.\frac{\partial\tilde{f}}{\partial(x_1,x_2,x_3)}\right|_{\substack{x_1=x_1^*\\x_2=x_2^*\\x_3=x_3^*}}=\begin{pmatrix}-2\cdot\frac{\left(f_p+\frac{1}{\overline{G_0}^2}\right)\cdot x_1^*}{T_{WP}} & \frac{1}{T_{WP}} & 0\\ -\frac{1}{C_s} & 0 & \frac{1}{C_s}\\ 0 & -\frac{1}{T_{WC}} & -2\cdot\frac{f_p\cdot x_3^*}{T_{WC}}\end{pmatrix}$$

The characteristic equation has all its roots with real negative parts and hence the system is linearly asymptotically stable near the equilibrium point. This means that the zero dynamics of the nonlinear system is stable in a neighbourhood of the origin.

5.4.3 Comparative Studies Using $f_{cost(A)}$

In this subsection comparative studies of the behaviour of five different controllers (PID, PI-PD, Gain Scheduling PI-PD, NL C and NL D) are presented. Similarly to the case presented in Subsection 5.3.5, the studies are done for different operating points defined by the disturbance $\overline{P}_{load}$ (non-frequency-sensitive load).

The values of the weight coefficients of the cost function (5. 10) have the same values taken for the nonlinear controller applied to the hydraulic turbine model *with no surge tank*.

In these studies the parameters from IEEE Working Group (1992), i.e. the Parameters 1 in Table 3.5 Chapter 3, are used.

5.4.3.1 Comparison of Rotor Speed Behaviour for Different Load Changes

The parameters of the controllers PID, PI-PD, NL C and NL D are adjusted according to the minimal value of the cost function after applying a step function on the disturbance $\overline{P}_{load}$ from 0.8 [pu] to 0.9 [pu].

This operating point corresponds to the worst case for controllers with fixed parameters. Table 5.6 shows the parameter values of the PID, PI-PD, NL C and NL D controllers, which are obtained after this adjustment.

Controller	K_p	K_i	K_d	K_{p1}	R_p	R_3	R_4	$f_{cost(A)}$
PI-PD	1	0.04	5	1	0	-	-	590
PID	2.5	0.05	2	-	0	-	-	596
NL C	1	1	-	-	-	35	-	1670
NL D	1	0.75	40	1	-	-	60	530

Table 5.6: Parameters of the PI-PD, PID, NL C and NL D controllers.

Figure 5.31 shows the rotor speed response for the disturbance $\overline{P}_{load}$ from 0.8 to 0.9 [pu].

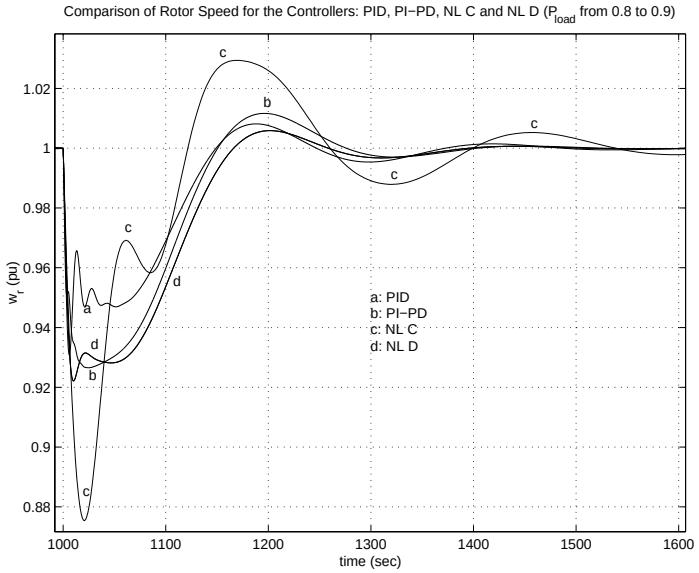

Figure 5.31: Comparison of rotor speed.

5.4.3.2 Comparison of Cost Function Values $f_{cost(A)}$

Figure 5.32 shows the cost function for the PID, PI-PD, Gain Scheduling PI-PD and NL D controllers for different operating points.

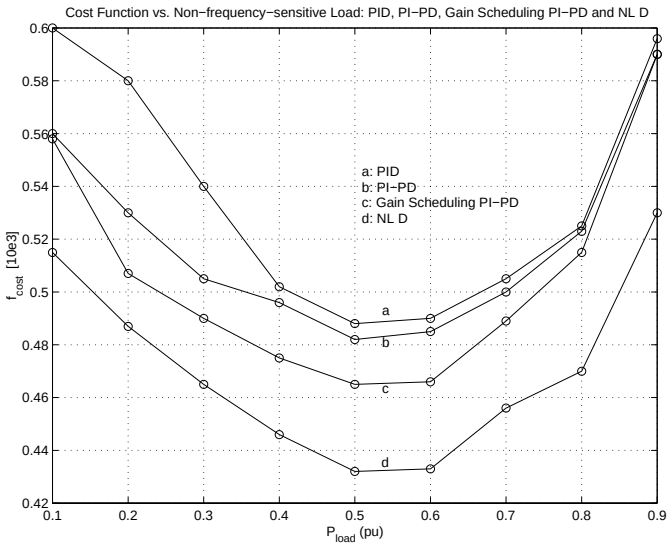

Figure 5.32: Comparison of cost function for the controllers PID, PI-PD, Gain Scheduling PI-PD and NL D ($f_{cost(A)}$).

The values of the cost function ($f_{cost(A)}$) of the controller NL D are the lowest for all the operating points. Moreover, these values are 10 to 13 per cent lower than the Gain Scheduling PI-PD case. Therefore, the controller NL D produces a good dynamic behaviour with the most reduced wear in the gate servos.

5.4.4 Controller Adjustment Surfaces Using $f_{cost(A)}$

Once more, this subsection presents fine adjustments for the controllers. The 3-D graphics show a level surface where the minimum can be found.

5.4.4.1 Adjustment for the PI-PD Controller

For this case the represented level surface is $f_{cost(A)} = f(K_p, K_i)$, with $K_d = 5$.

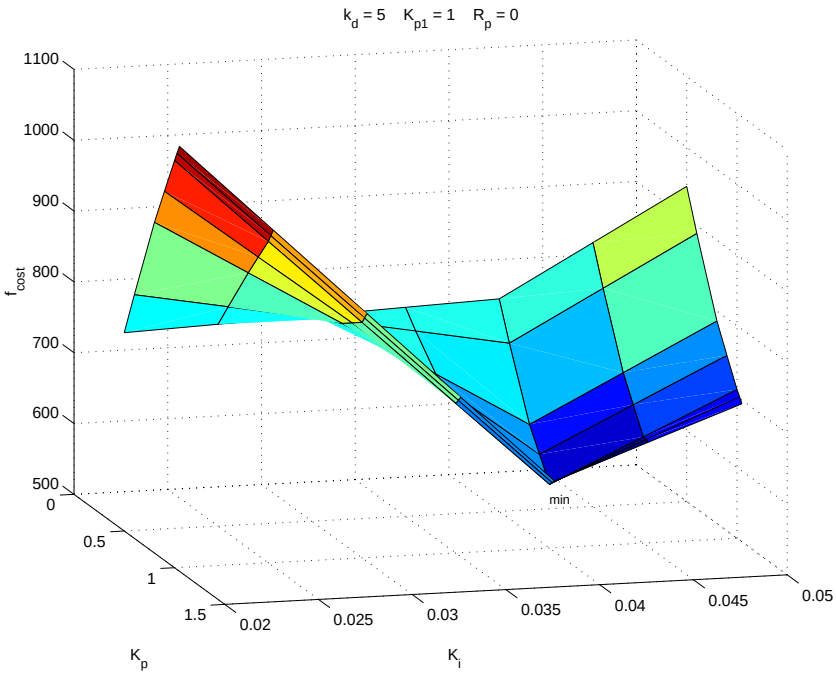

Figure 5.33: Adjustment surface for the PI-PD controller ($f_{cost(A)}$).

Figures 5.34 and 5.35 present transversal cuts in order to show the minimal value.

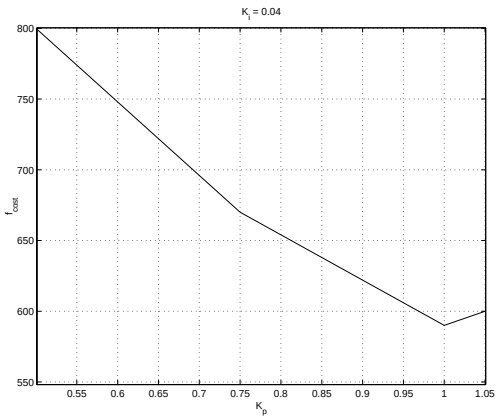

Figure 5.34: Plane $K_i = 0.04$

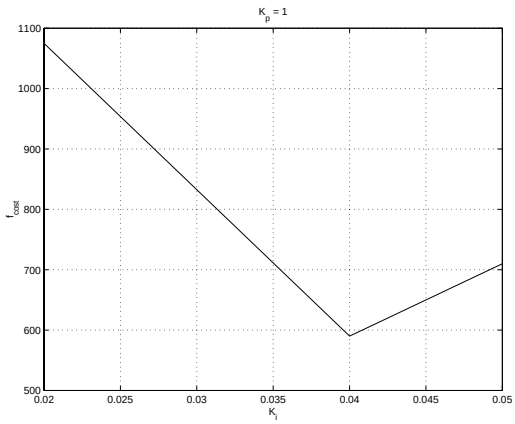

Figure 5.35: Plane $K_p = 1$

5.4.4.2 Adjustment for the Nonlinear Controller NL D

This controller has a PI-PD structure; therefore, its cost function is $f_{cost(A)} = f(K_p, K_i, K_d)$. In Figure 5.36 a level surface of $f_{cost(A)} = f(K_p, K_i)$, with $K_d = 40$ is depicted.

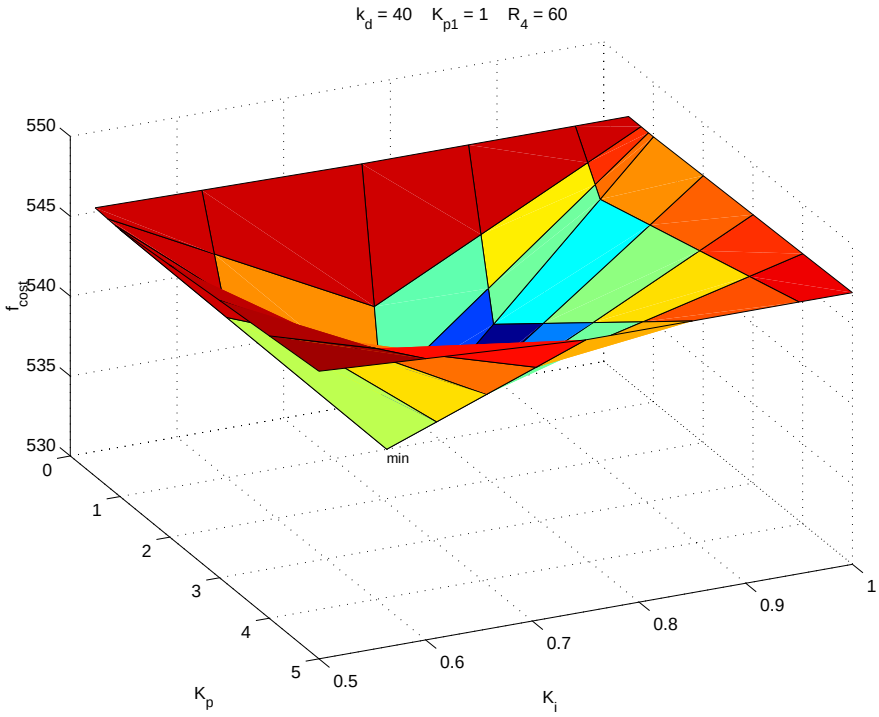

Figure 5.36: Adjustment surface for the controller NL D ($f_{cost(A)}$).

Figures 5.37 and 5.38 present transversal cuts with different planes to present the minimal value.

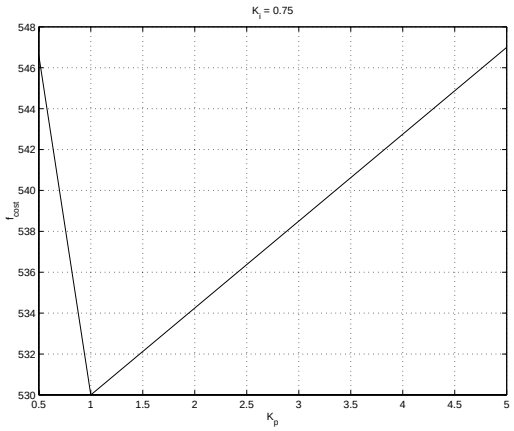

Figure 5.37: Plane $K_i = 0.75$

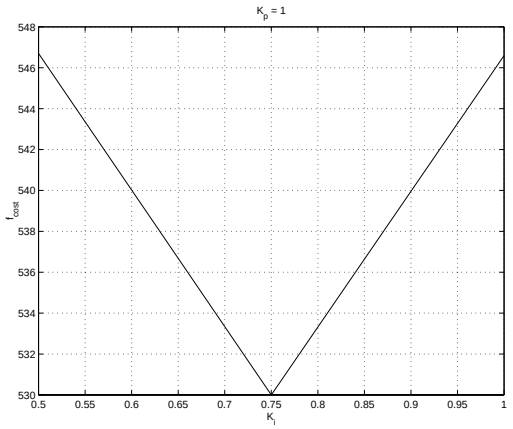

Figure 5.38: Plane $K_p = 1$

5.4.5 Comparative Studies Using $f_{cost(B)}$

This subsection presents comparative studies of the behaviour for the PID, PI-PD, Gain Scheduling PI-PD and NL D controllers using the cost function $f_{cost(B)}$.

The values of the weight coefficients of the cost function of equation (5. 11) have the same values considered for the nonlinear controller applied to the hydraulic turbine model *with no surge tank.*

Once again, the parameters of the PID, PI-PD, NL C and NL D controllers are adjusted according to the minimal value of the cost function after applying a step function on the disturbance $\overline{P}_{load}$ from 0.8 [pu] to 0.9 [pu].

This operating point corresponds to the worst case for a controller with fixed parameters. Table 5.7 shows the values of the parameters of the PID, PI-PD, NL C and NL D controllers found after this adjustment.

Controller	K_p	K_i	K_d	K_{p1}	R_p	R_3	R_4	$f_{cost(B)}$
PI-PD	1	0.04	5	1	0	-	-	7.35
PID	1.25	1.5	0	-	0	-	-	7.40
NL C	1	1	-	-	-	35	-	11.258
NL D	0.25	0.75	40	1	-	-	40	6.245

Table 5.7: Parameters of the PI-PD, PID, NL C and NL D controllers.

5.4.5.1 Comparison of Cost Function Values $f_{cost(B)}$

Figure 5.39 shows the values of the cost function ($f_{cost(B)}$) of the PID, Gain Scheduling PI-PD, NL C and NL D controllers for different operating points.

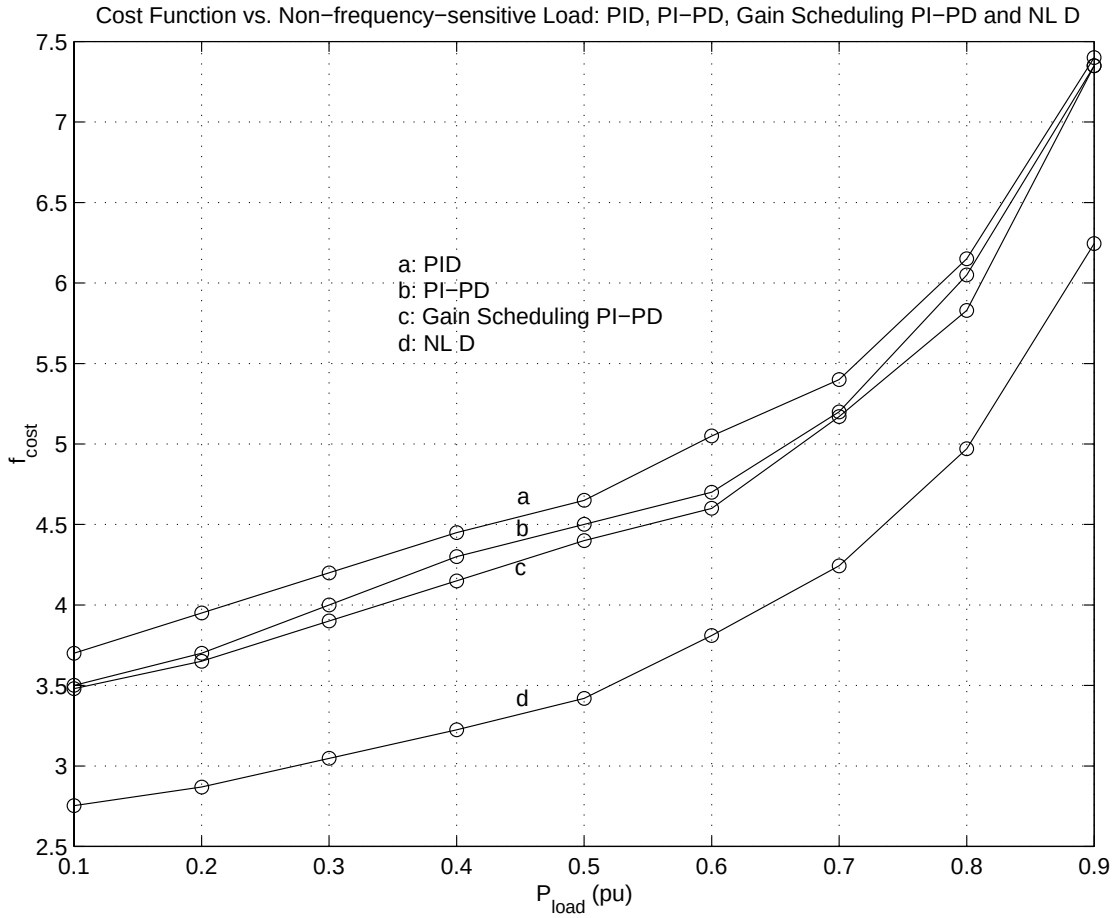

Figure 5.39: Comparison of cost function for the controllers: PID, PI-PD and NL D ($f_{cost(B)}$).

The values of the cost function ($f_{cost(B)}$) in the case of the controller NL D are the lowest for all operating points. Moreover, the values of the controller NL D are 15 to 21 per cent lower than the values of the Gain Scheduling PI-PD. Therefore, the controller NL D produces a good quality dynamic behaviour by reducing wear in the gate servos.

5.4.6 Controller Adjustment Surfaces Using $f_{cost(B)}$

This subsection shows fine adjustments for the controllers by means of 3-D graphics where the minimum may be found.

5.4.6.1 Adjustment for the PI-PD Controller

For this case the represented level surface is $f_{cost(B)} = f(K_p, K_i)$, with $K_d = 5$.

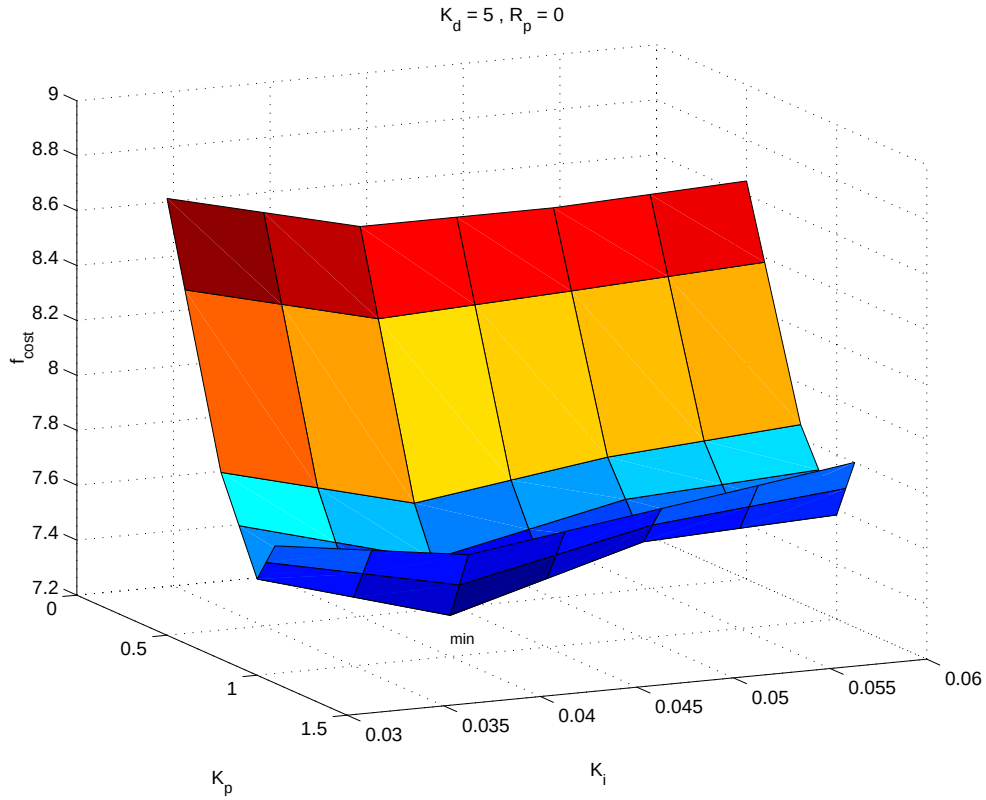

Figure 5.40: Adjustment surface for the PI-PD controller ($f_{cost(B)}$).

Figures 5.41 and 5.42 present transversal cuts with different planes where the minimal value is shown.

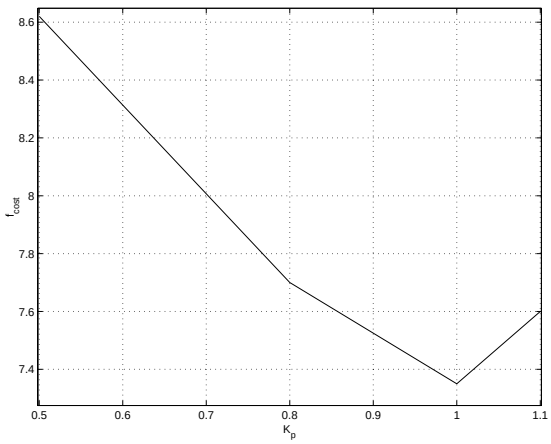

Figure 5.41: Plane $K_i = 0.04$

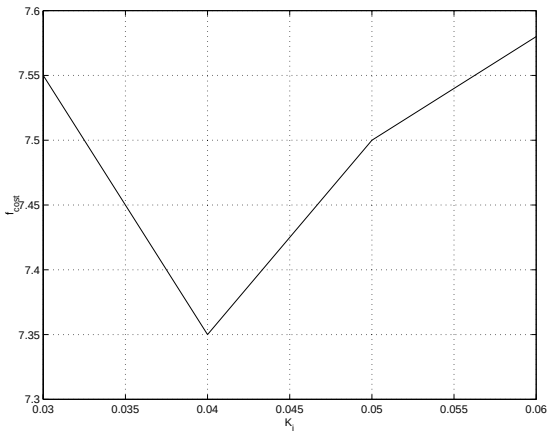

Figure 5.42: Plane $K_p = 1$

5.4.6.2 Adjustment for the Nonlinear Controller NL D

This controller is based on the PI-PD; therefore, its cost function is $f_{cost} = f(K_p, K_i, K_d)$. In Figure 5.43 is depicted a level surface of $f_{cost(B)} = f(K_p, K_i)$ with K_d=40.

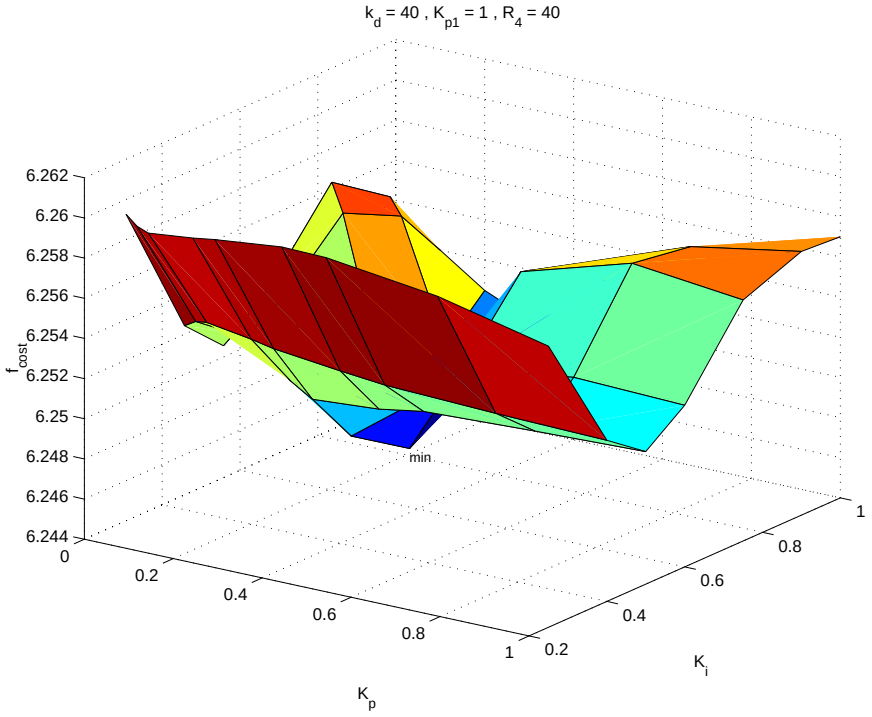

Figure 5.43: Adjustment surface for the controller NL D ($f_{cost(B)}$).

Figures 5.44 and 5.45 present transversal cuts with different planes to illustrate the minimal value.

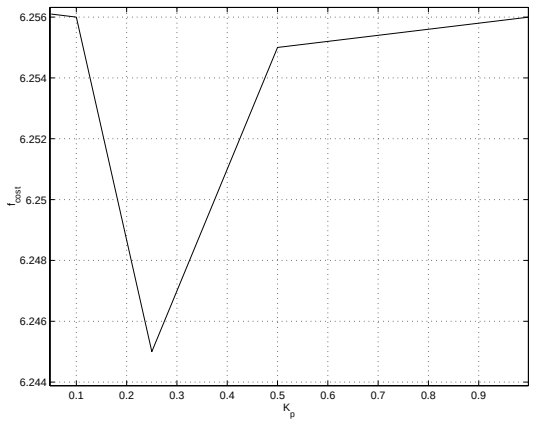

Figure 5.44: Plane K_i = 0.75

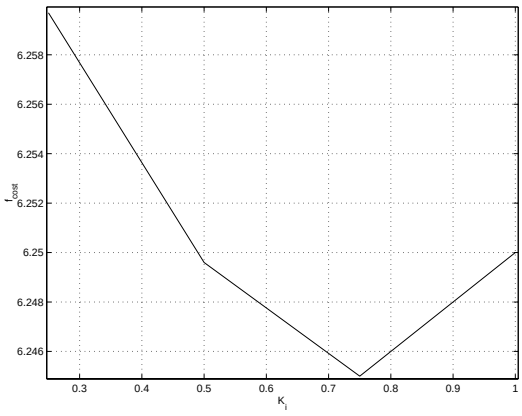

Figure 5.45: Plane K_p = 0.25

5.5 Load Rejection Studies

The hydroelectric power plant may suddenly reject load during steady state operation due to some disturbances, e.g. a failure causes that protections disconnect some loads supply by the unit, hence the load is reduced and the controller actuates in order to recuperate the nominal value of the rotor speed. This is an important study and is performed for the nonlinear controllers proposed in this chapter.

Moreover, the comparison of the rotor speed for different loads are presented, as well as two figures where the cost function $f_{cost(A)}$ versus discrete increments of non-frequency-sensitive load ($\Delta\overline{P}_{load}$) is represented.

5.5.1 Study for the Controller NL B

Figure 5.46 depicts the load rejection study of the nonlinear controller NL B for three different loads.

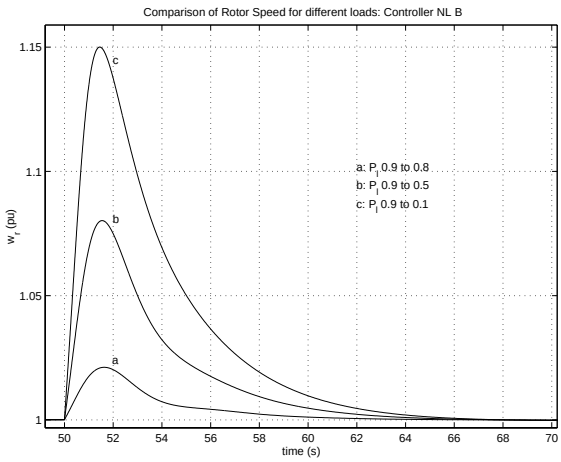

Figure 5.46: Load rejection study of the controller NL B for three different loads.

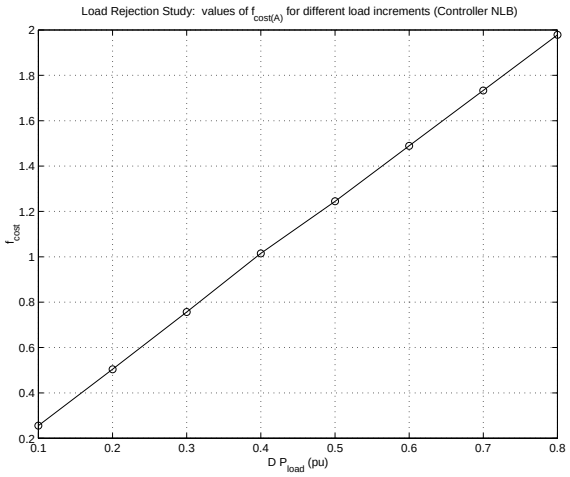

Figure 5.47: Representation of the relation between $f_{cost(A)}$ and $\Delta\overline{P}_{load}$.

Figure 5.47 shows an interesting “linear” relation between $f_{cost(A)}$ and $\Delta\overline{P}_{load}$. This relation can be explained by the fact that there is not surge tank effects and the controller reaches the steady state speedily.

5.5.2 Study for the Controller NL D

Figure 5.48 depicts the load rejection study of the nonlinear controller NL D for two different loads.

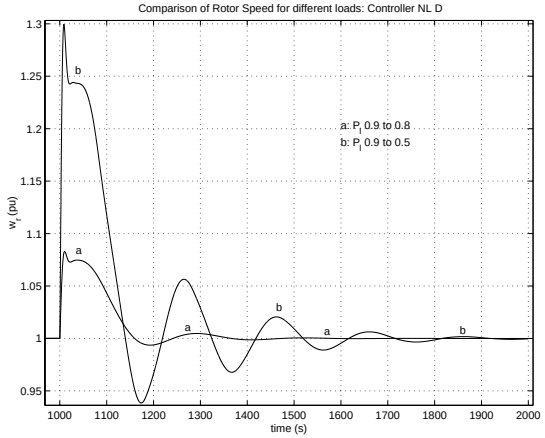

Figure 5.48: Load rejection study of the controller NL D for two different loads.

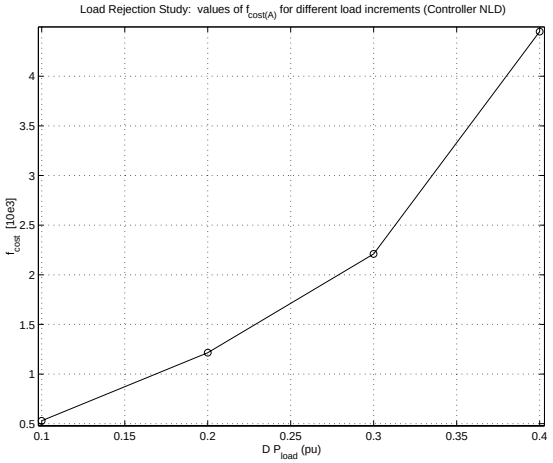

Figure 5.49: Graphic of the relation between $f_{cost(A)}$ and $\Delta\overline{P}_{load}$.

In Figure 5.49 the "quadratic" relation between $f_{cost(A)}$ and $\Delta\overline{P}_{load}$ is depicted. This is due to the effects of the surge tank and the cost function $f_{cost(A)}$ that penalises large values of time and its duration.

5.6 Summary and Conclusions

This chapter has presented the design of nonlinear controllers from nonlinear models (with or without surge tank effects) of hydroelectric power plants that work in an isolated system. A mixed structure of nonlinear techniques based on differential geometry and the PI or PI-PD controllers proved to give good results (Quiroga, Batlle and Riera, 2000). This technique is applied to the design of nonlinear controllers from models of hydroelectric power plants with surge tank effects.

Nonlinear Controllers designed from Nonlinear Models *with no* Surge Tank Effects

For nonlinear controllers designed from nonlinear models with no surge tank effects, Section 5.3 has presented an updating of the comparison studies (Quiroga, Batlle and Riera, 2000) by including the behaviour of the PI-PD and Gain Scheduling PI-PD controllers. The realistic cost function ($f_{cost(A)}$) penalises the speed error, its duration and long periods of time; moreover, it penalises the gate movements, and specially its duration and those that extend during long periods of time. This function is used to evaluate the performance of the controllers. Controller NL B shows the best performance, and its cost function has an average value of 15 per cent lower than the value of the Gain Scheduling PI-PD controller.

The cost function ($f_{cost(B)}$) penalises the speed error and its duration, and the gate movement and its duration. The values of the $f_{cost(B)}$ for the controller NL B are the lowest for all operating points and are between 10 to 13 per cent lower than the values of the Gain Scheduling PID controller.

Moreover, it is demonstrated that using both $f_{cost(A)}$ and $f_{cost(B)}$, the nonlinear controller NL B exhibits the best behaviour.

The load rejection study for the controller NL B shows that the relation between $f_{cost(A)}$ and $\Delta\overline{P}_{load}$ is “linear”. This relation can be explained by the fact that there are no surge tank effects and the controller reaches the steady state speedily.

Nonlinear Controllers designed from Nonlinear Models *with* Surge Tank Effects

Section 5.4 has presented the design and comparison studies of conventional PID with two nonlinear controllers (NL C and NL D) based on the partial state feedback linearization technique and a PI or PI-PD structure.

The Controller NL D has displayed the best performance since the cost function ($f_{cost(A)}$) has an average value of 12 per cent lower than the values of the Gain Scheduling PI-PD, moreover it is 15 per cent lower than the values of the PID.

The values of the $f_{cost(B)}$ for the controller NL D are also the lowest at all operating points, the values of the NL D are between 15 to 21 per cent lower than the values of the Gain

Scheduling PI-PD. It is demonstrated that utilising both $f_{cost(A)}$ and $f_{cost(B)}$, the nonlinear controller NL D has the best behaviour.

It is observed that for the controllers Gain Scheduling PI-PD, PI-PD, PID and NL D the values of the cost function ($f_{cost(B)}$) increase when the values of the load ($\overline{P}_{load}$) increase. On the other hand the curves of the cost function ($f_{cost(A)}$) versus non-frequency-sensitive-load ($\overline{P}_{load}$) for the same Gain Scheduling PI-PD, PI-PD, PID and NL D controllers, have a parabolic shape due to the penalisation of large time values considered in $f_{cost(A)}$.

The load rejection study for the controller NL D shows that the relation between $f_{cost(A)}$ and $\Delta\overline{P}_{load}$ is “quadratic”. This is due to the effects of the surge tank and the fact that the cost function $f_{cost(A)}$ penalises large values of time and time duration.